

The electroweak standard model

José I. Illana

Departamento de Física Teórica y del Cosmos, Universidad de Granada, E-18071 Granada, Spain.

Received 31 December 2021; accepted 17 February 2022

After introducing the basic symmetry principles, the full lagrangian of the Standard Model of the electroweak interactions is derived in detail and the most relevant aspects of its phenomenology are discussed, with special emphasis on the determination of the input parameters and the consistency checks of the model.

Keywords: Electroweak standard model.

DOI: <https://doi.org/10.31349/SuplRevMexFis.3.020721>

1. Fields and symmetries

1.1. Basics: Poincaré symmetry

1.1.1. Guided by symmetry

Relativistic quantum field theory (QFT) reconciles quantum mechanics and special relativity [1–6]. Relativistic fields are irreducible representations (irreps) of the Poincaré group, including Lorentz transformations (space rotations and Lorentz boosts) and spacetime translations. Examples of field irreps are the scalar $\phi(x)$, the four-vector $V_\mu(x)$ and the symmetric tensor $h_{\mu\nu}(x)$, where $\mu, \nu \in \{0, 1, 2, 3\}$ are Lorentz indices. The Lorentz subgroup is locally isomorphic to $SU(2) \otimes SU(2)$ whose irreps are labeled by (j_-, j_+) so it also admits spinorial representations where j_\pm can be half-integer, as for example the Weyl bispinor fields $\psi_L(x) \sim (1/2, 0)$ and $\psi_R(x) \sim (0, 1/2)$ that are two non-equivalent (conjugated) representations of spin $j = 1/2$ under rotations. The Dirac four-spinor field $\psi(x) = \psi_L(x) \oplus \psi_R(x)$ is a reducible representation of the Lorentz group containing left and right-handed chiralities, exchanged by a parity transformation.

To describe the field dynamics one introduces the action

$$S[\phi_i] = \int d^4x \mathcal{L}(\phi_i(x), \partial_\mu \phi_i(x)), \quad (1)$$

where the lagrangian (density) $\mathcal{L}(x) = \mathcal{L}(\phi_i, \partial_\mu \phi_i)$ is a local function of the fields and their derivatives, and ϕ_i stands for any type of fields (ϕ, ψ, V_μ , etc.). The action must be invariant under Poincaré transformations according to the covariance principle of special relativity. As an example, the lagrangian of a free Dirac field $\psi(x)$ is

$$\mathcal{L}_0 = \bar{\psi}(i\not{\partial} - m)\psi, \quad (2)$$

where γ^μ are the Dirac or ‘gamma’ matrices, $\not{\partial} \equiv \gamma^\mu \partial_\mu$ (slash notation), $\bar{\psi} \equiv \psi^\dagger \gamma^0$ is the Dirac adjoint and the constant m is the Dirac mass.

The lagrangian contains all the information about the particular theory under study. Following Noether’s (first) theorem, any continuous global symmetry of the action is in correspondence with a conservation law. In particular, the con-

servation of energy, linear momentum and angular momentum are the consequence of the invariance under time translations, space translations and space rotations, respectively, all of which are Poincaré symmetries.

Given a lagrangian, one derives the equations of motion (Euler-Lagrange equations), which describe the classical evolution of the fields. They are obtained from the principle of least action: the field configuration must be a stationary point of the action, *i.e.* $\delta S = 0$. Then

$$\begin{aligned} \delta S &= \int d^4x \sum_i \left(\frac{\partial \mathcal{L}}{\partial \phi_i} \delta \phi_i + \frac{\partial \mathcal{L}}{\partial (\partial_\mu \phi_i)} \delta (\partial_\mu \phi_i) \right) \\ &= \int d^4x \sum_i \left(\frac{\partial \mathcal{L}}{\partial \phi_i} - \partial_\mu \frac{\partial \mathcal{L}}{\partial (\partial_\mu \phi_i)} \right) \delta \phi_i = 0, \end{aligned} \quad (3)$$

where we have used integration by parts and dropped the boundary term under the assumption that field variations vanish at infinity. Since (3) must hold for any variation $\delta \phi_i$, we get for each field the corresponding equation of motion (EoM):

$$\frac{\partial \mathcal{L}}{\partial \phi_i} - \partial_\mu \frac{\partial \mathcal{L}}{\partial (\partial_\mu \phi_i)} = 0. \quad (4)$$

For instance, in the case of a free Dirac field, the EoM is the well-known Dirac equation,

$$(i\not{\partial} - m)\psi(x) = 0, \quad (5)$$

whose general solution is

$$\begin{aligned} \psi(x) &= \int \frac{d^3p}{(2\pi)^3 \sqrt{2E_p}} \\ &\times \sum_{s=1,2} \left(a_{\mathbf{p},s} u^{(s)}(p) e^{-ip \cdot x} + b_{\mathbf{p},s}^* v^{(s)}(p) e^{ip \cdot x} \right), \end{aligned} \quad (6)$$

with $p^2 = E_p^2 - |\mathbf{p}|^2 = m^2$, where $u^{(s)}(p)$ and $v^{(s)}(p)$ are constant four-spinors of positive and negative energy, respectively ($\pm E_p$ with $E_p \equiv +\sqrt{|\mathbf{p}|^2 + m^2}$) verifying

$$\begin{aligned} (\not{p} - m)u^{(s)}(p) &= 0, \\ (\not{p} + m)v^{(s)}(p) &= 0, \quad s = 1, 2, \end{aligned} \quad (7)$$

and $a_{\mathbf{p},s}, b_{\mathbf{p},s}$ are for the moment just complex coefficients with convenient normalizations.ⁱ

1.1.2. Quantization

To quantize a classical theory à la canonical, we need to have a well-defined hamiltonian formulation of the theory. First we compute the conjugate momenta of every field, $\Pi_i(x) = \partial\mathcal{L}/\partial(\partial_0\phi_i)$, then we perform the Legendre transform of the lagrangian with respect to the velocities $\dot{\phi}_i = \partial_0\phi_i$ and finally we invert the definition of canonical momenta to express the velocities in terms of them. The resulting object is the hamiltonian (density),

$$\mathcal{H}(x) = \sum_i \Pi_i \dot{\phi}_i - \mathcal{L}(x). \quad (8)$$

Once the theory is written in terms of fields and conjugate momenta, the canonical quantization proceeds as follows:

1. Promote the fields and canonical momenta to *operators* acting on a certain Hilbert space.
2. Impose the canonical *quantization rules*. These are either commutation or anticommutation relations between the fields and their conjugate momenta at equal times. Which rules must be imposed depends on what is the type of fields (bosonic or fermionic), and correspond to those leading to a hamiltonian bounded from below, so for a consistent theory one cannot freely choose. For instance, in the case of the Dirac fermion field we have to use anticommutators,

$$\begin{aligned} \{a_{\mathbf{p},r}, a_{\mathbf{k},s}^\dagger\} &= \{b_{\mathbf{p},r}, b_{\mathbf{k},s}^\dagger\} = (2\pi)^3 \delta^3(\mathbf{p} - \mathbf{k}) \delta_{rs}, \\ \{a_{\mathbf{p},r}, a_{\mathbf{k},s}\} &= \{b_{\mathbf{p},r}, b_{\mathbf{k},s}\} = 0. \end{aligned} \quad (9)$$

As a consequence, $a_{\mathbf{p},s}$, $b_{\mathbf{p},s}$ (and their hermitian adjoints) become operators that annihilate (create) fermionic modes of well-defined momentum \mathbf{p} , mass m and spin component s on the Fock space of multiparticle states that we call particles and antiparticles, respectively. The vacuum $|0\rangle$ is defined by $a_{\mathbf{p},s}|0\rangle = b_{\mathbf{p},s}|0\rangle = 0$; the states with one particle or antiparticle (conveniently normalized) are given by

$$\begin{aligned} \text{one particle} &\equiv \sqrt{2E_{\mathbf{p}}} a_{\mathbf{p},s}^\dagger |0\rangle, \\ \text{one antiparticle} &\equiv \sqrt{2E_{\mathbf{p}}} b_{\mathbf{p},s}^\dagger |0\rangle, \end{aligned} \quad (10)$$

and general fermionic multiparticle states are of the form $a_{\mathbf{p}_1,s_1}^\dagger a_{\mathbf{p}_2,s_2}^\dagger \cdots b_{\mathbf{q}_1,r_1}^\dagger b_{\mathbf{q}_2,r_2}^\dagger \cdots |0\rangle$. Hence they are antisymmetric under the exchange of any pair (or symmetric if they were bosons) enforced by the quantization rules. This is the spin-statistics connection. Another consequence is causality: the commutation of two fields at points separated by a spacelike interval.

3. Apply *normal ordering* to the hamiltonian (and any observable made of fields): move all creation operators to the left of annihilation operators, adding a minus sign each time you exchange the position of any annihilation or creation operator if they are fermionic. This prescription subtracts the infinite contribution of the vacuum to the expectation value of the observable.

1.2. Global symmetries and gauge invariance

1.2.1. Internal symmetries and the gauge principle

The free lagrangian

The free lagrangian for the Dirac field (2) is invariant under spacetime (Poincaré) symmetries *and* also under ‘internal’ symmetries, acting only on the fields, not changing the spacetime coordinates. They consist of *global* U(1) phase transformations,

$$\psi(x) \mapsto e^{-iQ\theta} \psi(x), \quad (11)$$

where Q and θ are real constants. Then, as a consequence of Noether’s theorem, there must exist a divergentless current and a conserved charge associated to this continuous symmetry,

$$\partial_\mu \mathcal{J}^\mu = 0, \quad \partial_t \mathcal{Q} = 0 \quad \text{with} \quad \mathcal{Q} = \int d^3x \mathcal{J}^0. \quad (12)$$

The Noether’s current corresponding to the U(1) invariance of the lagrangian is

$$\mathcal{J}^\mu = Q \bar{\psi} \gamma^\mu \psi. \quad (13)$$

After field quantization, the conserved charge becomes an operator on Fock space,

$$\begin{aligned} \mathcal{Q} &= Q \int d^3x : \bar{\psi} \gamma^0 \psi : \\ &= Q \int \frac{d^3p}{(2\pi)^3} \sum_{s=1,2} (a_{\mathbf{p},s}^\dagger a_{\mathbf{p},s} - b_{\mathbf{p},s}^\dagger b_{\mathbf{p},s}), \end{aligned} \quad (14)$$

where we have applied the normal ordering prescription for fermionic operators. From this we can easily check that particles and antiparticles carry opposite charges $\pm Q$:

$$\begin{aligned} \mathcal{Q} a_{\mathbf{k},r}^\dagger |0\rangle &= +Q a_{\mathbf{k},s}^\dagger |0\rangle \quad (\text{particle}), \\ \mathcal{Q} b_{\mathbf{k},s}^\dagger |0\rangle &= -Q b_{\mathbf{k},s}^\dagger |0\rangle \quad (\text{antiparticle}). \end{aligned} \quad (15)$$

Gauge invariance dictates interactions

It is evident that the free lagrangian is not invariant under phase transformations where $\theta = \theta(x)$, different for every spacetime point,

$$\psi(x) \mapsto e^{-iQ\theta(x)} \psi(x). \quad (16)$$

In order to impose that physics is invariant under these *local* or *gauge* U(1) transformations it is enough to perform the minimal substitution

$$\partial_\mu \rightarrow D_\mu = \partial_\mu + ieQA_\mu, \quad (17)$$

that introduces a *gauge field* $A_\mu(x)$ transforming as

$$A_\mu(x) \mapsto A_\mu(x) + \frac{1}{e} \partial_\mu \theta(x). \quad (18)$$

This basically ensures that $D_\mu \psi \mapsto e^{-iQ\theta(x)} D_\mu \psi$, so it transforms the same as ψ , hence the name of *covariant derivative*.

The outcome of this replacement is the generation of an interaction between ψ and A_μ given by the scalar product of the conserved current (13) and the gauge field,

$$\mathcal{L}_{\text{int}} = -e Q \bar{\psi} \gamma^\mu \psi A_\mu = -e \mathcal{J}^\mu A_\mu, \quad (19)$$

which is proportional to the coupling constant e (a property of the gauge field) and the conserved charge Q (a property of the fermion field).

Finally, we have to provide dynamics for the vector field we have introduced without spoiling gauge invariance. This is achieved by adding the following kinetic term,

$$\mathcal{L}_G = -\frac{1}{4} F_{\mu\nu} F^{\mu\nu}, \quad (20)$$

where $F_{\mu\nu} = \partial_\mu A_\nu - \partial_\nu A_\mu$ is a gauge invariant antisymmetric tensor, that has the same form as the electromagnetic tensor. In fact, applying the Euler-Lagrange equations for A_μ to the full invariant lagrangian ($\mathcal{L}_0 + \mathcal{L}_{\text{int}} + \mathcal{L}_G$),

$$\mathcal{L}_{\text{inv}} = \bar{\psi} (i\not{D} - m) \psi - \frac{1}{4} F_{\mu\nu} F^{\mu\nu}, \quad (21)$$

one obtains precisely Maxwell's equations, $\partial_\mu F^{\mu\nu} = e \mathcal{J}^\nu$, where $F^{\mu\nu}$ is the electromagnetic field strength and the four-current $\mathcal{J}^\mu = (\rho, \mathbf{j})$ includes the electric charge-density and charge-current in units of e .

We have seen that making local a global symmetry requires the existence of interactions, of a type that is determined by the symmetry. This way of introducing the interactions is known as the *gauge principle*.

A very important comment is here in order. We often call *gauge symmetry* to a local transformation of the fields with $\theta = \theta(x)$ that leaves invariant the lagrangian. Although this gauge invariance implies the existence of a global symmetry, which can be properly called a 'symmetry', with physical consequences like charge conservation, a local transformation is *not a symmetry* of our system, but a *redundancy* of our description of physics: we can redefine fields at every point of spacetime with no physical consequences. The gauge invariance is necessary to have a local description of massless spin-1 particles (two degrees of freedom) with four-vector fields, which are Lorentz invariant objects with too many polarizations. The gauge symmetry is more a gauge *freedom*.

The gauge principle in non-abelian gauge theories

Next we will apply the gauge principle to a more general symmetry group than just U(1). A general gauge symmetry group G is a compact N -dimensional Lie group, whose elements

$$g \in G, \quad g(\boldsymbol{\theta}) = e^{-iT_a \theta^a}, \quad a = 1, \dots, N, \quad (22)$$

are given by a set of real and continuous parameters $\{\theta^a\}$ in terms of N generators $\{T_a\}$ that form the basis of the Lie algebra of the group. The generators T_a of gauge groups are hermitian if the transformation is unitary, and in general the Lie algebra structure is totally determined by the commutators between the elements of the basis,

$$[T_a, T_b] = i f_{abc} T_c, \quad (23)$$

with f_{abc} the structure constants characterizing the group. The structure constants vanish if and only if the group is abelian (recall the Baker-Campbell-Hausdorff formula).

The finite-dimensional irreducible representations of a compact Lie group are unitary: the $g(\boldsymbol{\theta})$ are represented by unitary $d \times d$ matrices $U(\boldsymbol{\theta})$ that are expressed in terms of the corresponding Lie algebra representation of $\{T_a\}$. These matrices act on some d -dimensional vector space whose elements are called d -multiplets,

$$\Psi(x) \mapsto U(\boldsymbol{\theta}) \Psi(x), \quad \Psi = \begin{pmatrix} \psi_1 \\ \vdots \\ \psi_d \end{pmatrix}. \quad (24)$$

In our context, the multiplet components are fields.

Examples of Lie groups that often appear in quantum field theories are U(1) (abelian, with $N = 1$ generator) and SU(n), which is the group of $n \times n$ unitary matrices of unit determinant (non-abelian, with $N = n^2 - 1$ generators). The unitary irreps of abelian groups, like U(1), are one-dimensional. Prominent irreps of SU(n) groups are the 'fundamental representation' ($d = n$) and the 'adjoint representation' ($d = N$). The elements of the N -dimensional matrices representing the generators in the adjoint representation are $(T_a)_{bc} = -i f_{abc}$, totally antisymmetric for SU(n). Let us briefly list the main properties of these groups.

- U(1). The only generator is represented by a real number (Q), that labels each one-dimensional representation.
- SU(2). It has 3 generators. The structure constants are $f_{abc} = \epsilon_{abc}$ (Levi-Civita symbol). The generators in the fundamental representation ($d = 2$) can be chosen $T_a = \frac{1}{2} \sigma_a$, the 3 Pauli matrices. The adjoint representation has dimension 3.
- SU(3). It has 8 generators. The totally antisymmetric structure constants are given by $f_{123} = 1$, $f_{458} = f_{678} = \sqrt{3}/2$, $f_{147} = f_{156} = f_{246} = f_{247} = f_{345} = -f_{367} = 1/2$ and the others not related to these by permuting indices are zero. The generators in the fundamental representation can be chosen $T_a = (1/2) \lambda_a$, the 8 Gell-Mann matrices. The adjoint representation has dimension 8.

Consider now the free lagrangian for a fermion multiplet,

$$\mathcal{L}_0 = \bar{\Psi}(i\cancel{\partial} - m)\Psi, \quad (25)$$

invariant under an N -dimensional Lie group G of global transformations,

$$\Psi(x) \mapsto U(\boldsymbol{\theta})\Psi(x). \quad (26)$$

We can get a lagrangian invariant under local (gauge) transformations $\boldsymbol{\theta} = \boldsymbol{\theta}(x)$ by substituting the covariant derivative

$$\partial_\mu \rightarrow D_\mu = \partial_\mu - ig\widetilde{W}_\mu, \quad \widetilde{W}_\mu \equiv T_a W_\mu^a, \quad (27)$$

where one gauge field $W_\mu^a(x)$ per generator T_a has been introduced, transforming as

$$\widetilde{W}_\mu(x) \mapsto U\widetilde{W}_\mu(x)U^\dagger - \frac{i}{g}(\partial_\mu U)U^\dagger. \quad (28)$$

The first term implements the global transformation of a multiplet of N vector fields in the adjoint representation and the second accounts for the local dependence with the spacetime point x . Then $D_\mu\Psi \mapsto UD_\mu\Psi$, transforming the same as Ψ , just as we need. The choice of sign for the coupling g in the covariant derivative is conventional.

The new lagrangian contains interactions of fermions in Ψ with every W_μ^a ,

$$\mathcal{L}_{\text{int}} = g\bar{\Psi}\gamma^\mu T_a\Psi W_\mu^a = g\mathcal{J}_a^\mu W_\mu^a, \quad (29)$$

where each \mathcal{J}_a^μ is the Noether's current associated to the invariance of the lagrangian under the symmetry generated by T_a . The strength of the interaction of gauge field W_μ^a to two fermion fields ψ_i and ψ_j of the d -multiplet is proportional to the coupling g and is given by the element $(T_a)_{ij}$ of the corresponding generator in that representation. The fermion charges under group G are eigenvalues of the generators in the given representation. Fermion singlets belong to the trivial one-dimensional representation with $T_a = 0$ and hence do not couple to gauge fields.

The next step is to add kinetic terms for the gauge fields respecting the gauge invariance. Interestingly, this cannot be done without introducing at the same time interactions among the gauge fields when the symmetry is non-abelian. The minimal choice is the Yang-Mills lagrangian,

$$\mathcal{L}_{\text{YM}} = -\frac{1}{2}\text{Tr}\left\{\widetilde{W}_{\mu\nu}\widetilde{W}^{\mu\nu}\right\} = -\frac{1}{4}W_{\mu\nu}^a W^{a\mu\nu}, \quad (30)$$

where

$$\begin{aligned} \widetilde{W}_{\mu\nu} &\equiv T_a W_{\mu\nu}^a \equiv D_\mu\widetilde{W}_\nu - D_\nu\widetilde{W}_\mu \\ &= \partial_\mu\widetilde{W}_\nu - \partial_\nu\widetilde{W}_\mu - ig[\widetilde{W}_\mu, \widetilde{W}_\nu], \end{aligned} \quad (31)$$

from which one derives the field strengths:

$$W_{\mu\nu}^a = \partial_\mu W_\nu^a - \partial_\nu W_\mu^a + gf_{abc}W_\mu^b W_\nu^c. \quad (32)$$

These are a generalization of $F_{\mu\nu}$ to the non-abelian case. They transform in the adjoint representation of the gauge group,

$$\widetilde{W}_{\mu\nu} \mapsto U\widetilde{W}_{\mu\nu}U^\dagger. \quad (33)$$

Note that, besides the kinetic terms, \mathcal{L}_{YM} contains cubic and quartic self-interactions of gauge fields completely determined by the gauge group properties:

$$\begin{aligned} \mathcal{L}_{\text{kin}} &= -\frac{1}{4}(\partial_\mu W_\nu^a - \partial_\nu W_\mu^a)(\partial^\mu W^{a\nu} - \partial^\nu W^{a\mu}), \\ \mathcal{L}_{\text{cubic}} &= -\frac{1}{2}gf_{abc}(\partial_\mu W_\nu^a - \partial_\nu W_\mu^a)W^{b\mu}W^{c\nu}, \\ \mathcal{L}_{\text{quartic}} &= -\frac{1}{4}g^2 f_{abe}f_{cde}W_\mu^a W_\nu^b W^{c\mu}W^{d\nu}. \end{aligned} \quad (34)$$

The self-couplings of gauge fields in non-abelian theories have profound consequences. For instance, in quantum chromodynamics where gluons interact with each other, it is the main reason for confinement.

1.2.2. Quantization of gauge theories

So far we have discussed only classical gauge theories. If we now try to quantize the theory we encounter a problem: the propagator of the gauge field does not exist! The (Feynman) propagator is the basic correlator of the quantum field theory. It is a Green's function for the free equation of motion. For a scalar field,

$$D_F(x-y) = \int \frac{d^4p}{(2\pi)^4} \frac{i}{p^2 - m^2 + i\varepsilon} e^{-ip\cdot(x-y)}, \quad (35)$$

is indeed a Green's function (the analogue to the inverse) of the Klein-Gordon operator

$$(\square_x + m^2)D_F(x-y) = -i\delta^4(x-y), \quad (36)$$

or in momentum space,

$$\widetilde{D}_F(p) = \frac{i}{p^2 - m^2 + i\varepsilon}. \quad (37)$$

Similarly, the propagator of a fermion field,

$$S_F(x-y) = (i\cancel{\partial}_x + m) \int \frac{d^4p}{(2\pi)^4} \frac{i}{p^2 - m^2 + i\varepsilon} e^{-ip\cdot(x-y)}, \quad (38)$$

is a Green's function of the Dirac operator,

$$(i\cancel{\partial}_x - m)S_F(x-y) = i\delta^4(x-y), \quad (39)$$

or in momentum space,

$$\widetilde{S}_F(p) = \frac{i}{\cancel{p} - m + i\varepsilon}. \quad (40)$$

However, the propagator of a gauge field cannot be defined. For the simpler non-abelian case (Maxwell's lagrangian) the equation of motion is

$$\partial_\mu F^{\mu\nu} = [g^{\mu\nu}\square - \partial^\mu\partial^\nu]A_\mu = 0. \quad (41)$$

The Green's function should be the inverse of the differential operator in brackets, but this operator is not invertible because $-k^2 g^{\mu\nu} + k^\mu k^\nu$ is singular (it has a zero eigenvalue, with eigenvector k_μ). The origin of this problem is gauge invariance. The usual solution consists of modifying the lagrangian adding a gauge-fixing term, $\mathcal{L} = \mathcal{L}_G + \mathcal{L}_{GF}$, where in the so called R_ξ gauges

$$\mathcal{L}_{GF} = -\frac{1}{2\xi}(\partial^\mu A_\mu)^2. \quad (42)$$

The Euler-Lagrange equation of the modified lagrangian is then

$$\left[g^{\mu\nu} \square - \left(1 - \frac{1}{\xi}\right) \partial^\mu \partial^\nu \right] A_\mu = 0. \quad (43)$$

The propagator can now be computed in momentum space by inverting $-k^2 g^{\mu\nu} + (1 - \xi^{-1})k^\mu k^\nu$,

$$\tilde{D}_{\mu\nu}(k) = \frac{i}{k^2 + i\varepsilon} \left[-g_{\mu\nu} + (1 - \xi) \frac{k_\mu k_\nu}{k^2} \right], \quad (44)$$

where we have introduced the usual Feynman ε -prescription. Propagators are not physical observables, so the gauge dependence with the parameter ξ is not worrisome; it will cancel out in physical amplitudes. Particular cases of interest are the Landau gauge ($\xi = 0$) and the 't Hooft-Feynman gauge ($\xi = 1$). The latter has a simpler form, very helpful for loop calculations.

This procedure can be more easily justified in functional quantization. The gauge invariance of Maxwell's lagrangian under field transformations (18) implies that A_μ provides a redundant description of the electromagnetic field, because any four-vector in the same 'gauge orbit' leads to the same physics. As a consequence, we would be overcounting (infinite) equivalent configurations in the path integral, that leads to divergent Green's functions. To prevent this we impose a gauge condition, as $\partial^\mu A_\mu = 0$, and integrate only over one representative of each equivalence class. One can see that for an abelian gauge theory, like quantum electrodynamics, this constraint amounts to adding the gauge-fixing term (42).

However, in a non-abelian theory, like the electroweak standard model or quantum chromodynamics, a similar gauge-fixing,

$$\mathcal{L}_{GF} = -\sum_{a=1}^N \frac{1}{2\xi_a} (\partial^\mu W_\mu^a)^2, \quad (45)$$

is not enough. One also needs to add interactions with auxiliary fields called Faddeev-Popov ghosts, $c_a(x) = 1, \dots, N$, as many as gauge group generators,

$$\begin{aligned} \mathcal{L}_{FP} &= (\partial^\mu \bar{c}_a)(D_\mu^{\text{adj}})_{ab} c_b \\ &= (\partial^\mu \bar{c}_a)(\partial_\mu c_a - g f_{abc} c_b W_\mu^c), \end{aligned} \quad (46)$$

where we have introduced the covariant derivative in the adjoint representation,

$$D_\mu^{\text{adj}} = \partial_\mu - ig T_c^{\text{adj}} W_\mu^c, \quad (T_c^{\text{adj}})_{ab} = -if_{abc}. \quad (47)$$

This is merely a computational trick. The FP ghosts are unphysical, anticommuting scalar fields that only appear in loops as virtual particles, never as external legs of Feynman diagrams. They are produced in pairs and are needed in order to preserve the gauge symmetry at the quantum level. This procedure ensures that we do not count field configurations of W_μ^a which are pure gauge, nor count separately fields which differ only by a gauge transformation.

We finally know how to build the lagrangian of a quantum gauge field theory. Provided a gauge symmetry group and matter fields transforming in given group representations, the covariant derivatives specify the form of the interactions mediated by the gauge fields encoded in a gauge invariant piece \mathcal{L}_{inv} , that has to be supplemented by gauge-fixing terms and, if the symmetry group is non-abelian, by interactions with unphysical Faddeev-Popov ghosts,

$$\mathcal{L}_{\text{inv}} + \mathcal{L}_{GF} + \mathcal{L}_{FP}. \quad (48)$$

However, mass terms for the gauge fields break explicitly the gauge invariance. In fact the Proca lagrangian

$$\mathcal{L} = -\frac{1}{4} F_{\mu\nu} F^{\mu\nu} + \frac{1}{2} M^2 A_\mu A^\mu, \quad (49)$$

is not invariant under U(1) gauge transformations if $M \neq 0$, which on the other hand allows to define the propagator,

$$\tilde{D}_{\mu\nu}(k) = \frac{i}{k^2 - M^2 + i\varepsilon} \left(-g_{\mu\nu} + \frac{k^\mu k^\nu}{M^2} \right). \quad (50)$$

This is a serious issue if we wish to describe the fundamental interactions inspired by the gauge principle, since in particular weak interactions are mediated by massive gauge bosons. Fortunately, there is a way to cope with massive gauge mediators without spoiling the nice properties of the gauge symmetry, as we will see in next section.

1.3. Spontaneous symmetry breaking

1.3.1. Discrete symmetry

In order to understand the basic ideas behind the spontaneous symmetry breaking, let us first consider a real scalar field $\phi(x)$ with lagrangian

$$\mathcal{L} = \frac{1}{2} (\partial_\mu \phi)(\partial^\mu \phi) - V(\phi), \quad V(\phi) = \frac{1}{2} \mu^2 \phi^2 + \frac{\lambda}{4} \phi^4. \quad (51)$$

This lagrangian is invariant under a discrete \mathbb{Z}_2 symmetry $\phi \mapsto -\phi$. The hamiltonian is given by

$$\mathcal{H} = \frac{1}{2} (\dot{\phi}^2 + (\nabla\phi)^2) + V(\phi), \quad (52)$$

where the constants μ^2 and λ are real so that the hamiltonian is real/hermitian, and $\lambda > 0$ to ensure there exists a ground state. We distinguish two cases depending on the sign of μ^2 (Fig. 1). The interesting case is $\mu^2 < 0$ for which the minimum is not zero and degenerate, $\phi = v \equiv \pm \sqrt{-\mu^2/\lambda}$.

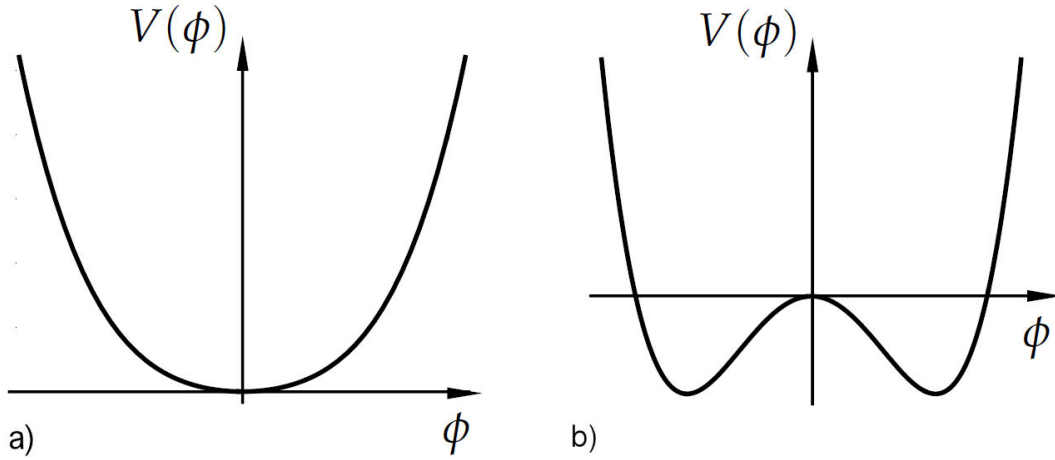


FIGURE 1. Potential symmetric under $\phi \mapsto -\phi$ for $\mu^2 > 0$ a) and $\mu^2 < 0$ b).

For a quantum field the configuration of minimum energy must be interpreted as the expectation value (VEV) of the field in the ground state, the vacuum. But if $\langle 0 | \phi | 0 \rangle = v \neq 0$ we have a problem, because $|0\rangle$ must be annihilated by any annihilation operator $a_{\mathbf{p}}$ in ϕ , a requirement for the construction of the Fock space of its multiparticle states. Therefore, we must perform a redefinition

$$\phi(x) \equiv v + \eta(x), \quad (53)$$

with $\eta(x)$ the field describing the quantum fluctuations, $\langle 0 | \eta | 0 \rangle = 0$. Then, at the quantum level, the same system is described by the following lagrangian in terms of $\eta(x)$:

$$\mathcal{L} = \frac{1}{2}(\partial_{\mu}\eta)(\partial^{\mu}\eta) - \lambda v^2 \eta^2 - \lambda v \eta^3 - \frac{\lambda}{4} \eta^4 + \frac{1}{4} \lambda v^4, \quad (54)$$

where η has a mass $\sqrt{2\lambda v^2}$. Note that the \mathbb{Z}_2 symmetry of the original lagrangian is broken, or hidden to be more precise. We say that the symmetry is ‘spontaneously’ broken because it is due to a non-invariant vacuum, not to an external agent. One may think that $\mathcal{L}(\eta)$ exhibits an ‘explicit’ breaking of the symmetry. However this is not the case: the fact that the coefficients of terms η^2 , η^3 and η^4 are not independent (they are determined by just two parameters, λ and v) is a remnant of the original symmetry. The last constant term can be omitted as it has no effect on the field dynamics.

1.3.2. Continuous global symmetry

Consider now a complex scalar field $\phi(x)$ with lagrangian

$$\begin{aligned} \mathcal{L} &= (\partial_{\mu}\phi)^{\dagger}(\partial^{\mu}\phi) - V(\phi), \\ V(\phi) &= \mu^2 \phi^{\dagger}\phi + \lambda(\phi^{\dagger}\phi)^2, \end{aligned} \quad (55)$$

which is invariant under global U(1) transformations $\phi \mapsto e^{-iQ\theta}\phi$. For $\lambda > 0$, $\mu^2 < 0$ (Fig. 2) the potential has a mexican hat shape with a degenerate minimum,

$$\langle 0 | \phi | 0 \rangle \equiv \frac{v}{\sqrt{2}}, \quad |v| = \sqrt{\frac{-\mu^2}{\lambda}}. \quad (56)$$

We may choose $v \in \mathbb{R}^+$ without loss of generality.ⁱⁱ In terms of the quantum fluctuations,

$$\begin{aligned} \phi(x) &\equiv \frac{1}{\sqrt{2}}[v + \eta(x) + i\chi(x)], \\ \langle 0 | \eta | 0 \rangle &= \langle 0 | \chi | 0 \rangle = 0, \end{aligned} \quad (57)$$

the lagrangian reads

$$\begin{aligned} \mathcal{L} &= \frac{1}{2}(\partial_{\mu}\eta)(\partial^{\mu}\eta) + \frac{1}{2}(\partial_{\mu}\chi)(\partial^{\mu}\chi) - \lambda v^2 \eta^2 \\ &\quad - \lambda v \eta(\eta^2 + \chi^2) - \frac{\lambda}{4}(\eta^2 + \chi^2)^2 + \frac{1}{4} \lambda v^4. \end{aligned} \quad (58)$$

Observe that the quantum lagrangian $\mathcal{L}(\eta, \chi)$ is no longer invariant under U(1). The spontaneous breaking of this symmetry leaves one massless scalar field, χ , whereas η has a mass proportional to the VEV, $m_{\eta} = \sqrt{2\lambda}v$.

In order to understand what are the consequences of the spontaneous breaking we will explore next the case of a group with more symmetries. Take an SO(3) triplet of real scalar fields, $\Phi(x)$, whose self-interactions are given by a similar mexican hat potential,

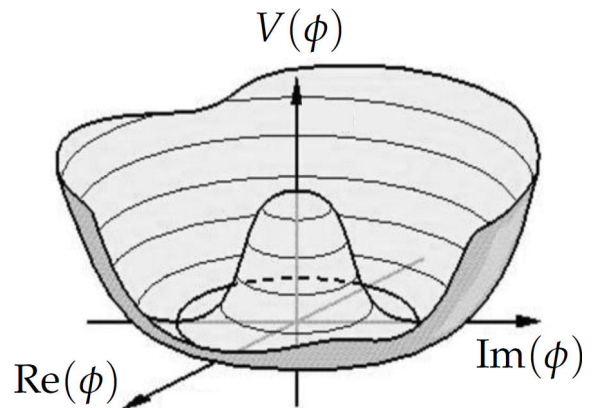


FIGURE 2. Mexican hat potential.

$$\mathcal{L} = \frac{1}{2}(\partial_\mu \Phi)^\top (\partial^\mu \Phi) - \frac{1}{2}\mu^2 \Phi^\top \Phi - \frac{\lambda}{4}(\Phi^\top \Phi)^2. \quad (59)$$

This theory is invariant under global SO(3) transformations $\Phi \mapsto e^{-iT_a \theta^a} \Phi$. For $\lambda > 0$, $\mu^2 < 0$ the triplet acquires a VEV

$$\langle 0 | \Phi^\top \Phi | 0 \rangle = v^2 = -\mu^2/\lambda. \quad (60)$$

We express the quantum field as $\Phi(x) \equiv (\varphi_1(x), \varphi_2(x), v + \varphi_3(x))^\top$ and define the complex combination $\varphi \equiv (1/\sqrt{2})(\varphi_1 + i\varphi_2)$. Then, the lagrangian can be rewritten as

$$\begin{aligned} \mathcal{L} = & (\partial_\mu \varphi)^\dagger (\partial^\mu \varphi) + \frac{1}{2}(\partial_\mu \varphi_3)(\partial^\mu \varphi_3) - \lambda v^2 \varphi_3^2 \\ & - \lambda v(2\varphi^\dagger \varphi + \varphi_3^2)\varphi_3 - \frac{\lambda}{4}(2\varphi^\dagger \varphi + \varphi_3^2)^2 + \frac{1}{4}\lambda v^4, \end{aligned} \quad (61)$$

which is not symmetric under SO(3) but is invariant under the U(1) transformation

$$\varphi \mapsto e^{-iQ\theta} \varphi \quad (Q \text{ is arbitrary}), \quad \varphi_3 \mapsto \varphi_3 \quad (Q = 0). \quad (62)$$

In other words, the group SO(3) has broken spontaneously into a U(1) subgroup. Since there are $3 - 1 = 2$ broken generators, 2 real scalar fields (or, equivalently, one complex scalar φ) remain massless, while the other scalar gets a mass proportional to the VEV:

$$m_{\varphi_1} = m_{\varphi_2} = 0 \quad (m_\varphi = 0), \quad m_{\varphi_3} = \sqrt{2\lambda}v. \quad (63)$$

The two examples we have just analyzed illustrate the *Goldstone's theorem* [7,8], the number of massless particles (*Nambu-Goldstone bosons*) is equal to the number of spontaneously broken generators of the symmetry. It is not difficult to understand what is behind this result. By definition of a symmetry, if the hamiltonian is invariant under the group G , we have

$$[T_a, H] = 0, \quad a = 1, \dots, N. \quad (64)$$

And by definition of the vacuum state,

$$H|0\rangle = 0 \quad \Rightarrow \quad H(T_a|0\rangle) = T_a H|0\rangle = 0. \quad (65)$$

Therefore:

- If $|0\rangle$ is such that $T_a|0\rangle = 0$ for all generators, there is a non-degenerate minimum: *the* vacuum, that will remain invariant.
- But if $|0\rangle$ is such that $T_{a'}|0\rangle \neq 0$ for some (broken) generators a' , there is a degenerate minimum: for any choice (*true* vacuum) we will have $e^{-iT_{a'}\theta^{a'}}|0\rangle \neq |0\rangle$, so it will not remain invariant. In this case there are excitations from $|0\rangle$ to $e^{-iT_{a'}\theta^{a'}}|0\rangle$ (flat directions of the potential) that cost no energy, so they correspond to massless particles (the Goldstone bosons).

1.3.3. Gauge symmetry

Take the simplest U(1) gauge invariant lagrangian for a complex scalar field $\phi(x)$:

$$\begin{aligned} \mathcal{L} = & -\frac{1}{4}F_{\mu\nu}F^{\mu\nu} + (D_\mu \phi)^\dagger (D^\mu \phi) - \mu^2 \phi^\dagger \phi - \lambda(\phi^\dagger \phi)^2, \\ D_\mu \equiv & \partial_\mu + ieQA_\mu, \end{aligned} \quad (66)$$

which is invariant under the transformations

$$\begin{aligned} \phi(x) & \mapsto e^{-iQ\theta(x)} \phi(x), \\ A_\mu(x) & \mapsto A_\mu(x) + \frac{1}{e}\partial_\mu \theta(x). \end{aligned} \quad (67)$$

If $\lambda > 0$ and $\mu^2 < 0$ the potential has a mexican hat shape with a minimum at $\langle 0 | \phi | 0 \rangle = v/\sqrt{2}$ where $|v| = \sqrt{-\mu^2/\lambda}$. We will choose $v \in \mathbb{R}^+$ as before. Then we write

$$\phi(x) \equiv \frac{1}{\sqrt{2}}[v + \eta(x) + i\chi(x)], \quad (68)$$

where η and χ are two real fields with null VEVs that describe particle excitations. In terms of these quantum fields the lagrangian reads

$$\begin{aligned} \mathcal{L} = & -\frac{1}{4}F_{\mu\nu}F^{\mu\nu} + \frac{1}{2}(\partial_\mu \eta)(\partial^\mu \eta) + \frac{1}{2}(\partial_\mu \chi)(\partial^\mu \chi) \\ & - \lambda v^2 \eta^2 - \lambda v \eta(\eta^2 + \chi^2) - \frac{\lambda}{4}(\eta^2 + \chi^2)^2 + \frac{1}{4}\lambda v^4 \\ & + eQvA_\mu \partial^\mu \chi + eQA_\mu(\eta \partial^\mu \chi - \chi \partial^\mu \eta) \\ & + \frac{1}{2}(eQv)^2 A_\mu A^\mu + \frac{1}{2}(eQ)^2 A_\mu A^\mu (\eta^2 + 2v\eta + \chi^2). \end{aligned} \quad (69)$$

Several comments are in order at this point:

- As expected, one of the scalar fields, χ , is massless (the Goldstone boson field) and the other one has a mass $m_\eta = \sqrt{2\lambda}v$. The global symmetry has broken spontaneously. We cannot say that the gauge symmetry has broken, because it is not really a symmetry, as we have discussed before.
- The gauge field A_μ acquires a mass $M_A = |eQv|$, proportional to the VEV of ϕ .
- There is a cross term $A_\mu \partial^\mu \chi$ that mixes A_μ and χ , producing kinetic terms that are neither diagonal nor invertible. Therefore, it is premature to infer the masses of A_μ and χ until we have made sense of this term.
- We still have to add a gauge-fixing term \mathcal{L}_{GF} .

The cross term can be removed and the gauge fixed at the same time by introducing the following gauge-fixing lagrangian:

$$\mathcal{L}_{\text{GF}} = -\frac{1}{2\xi}(\partial_\mu A^\mu - \xi M_A \chi)^2, \quad (70)$$

which in particular adds a term to the kinetic mixing above yielding an irrelevant total derivative, $M_A \partial_\mu (A^\mu \chi)$, that can be ignored. Therefore

$$\begin{aligned} \mathcal{L} + \mathcal{L}_{\text{GF}} = & -\frac{1}{4} F_{\mu\nu} F^{\mu\nu} + \frac{1}{2} M_A^2 A_\mu A^\mu - \frac{1}{2\xi} (\partial_\mu A^\mu)^2 \\ & + \frac{1}{2} (\partial_\mu \chi)(\partial^\mu \chi) - \frac{1}{2} \xi M_A^2 \chi^2 + \text{interactions}. \end{aligned} \quad (71)$$

The resulting propagators of A_μ and χ are, respectively:

$$\begin{aligned} \tilde{D}_{\mu\nu}(k) &= \frac{i}{k^2 - M_A^2 + i\epsilon} \left(-g_{\mu\nu} + (1 - \xi) \frac{k_\mu k_\nu}{k^2 - \xi M_A^2} \right), \\ \tilde{D}(k) &= \frac{i}{k^2 - \xi M_A^2 + i\epsilon}. \end{aligned} \quad (72)$$

This confirms that the interaction of A_μ with ϕ has provided the gauge boson with a mass proportional to $\langle 0 | \phi | 0 \rangle$. Notice also that χ has a gauge-dependent mass, an indication that it is not ‘physical’.

We can better understand the consequences of the spontaneous breaking of the symmetry in the context of a gauge theory if we use a more transparent parametrization of the quantum fluctuations of ϕ . Let us now define

$$\begin{aligned} \phi(x) &\equiv e^{iQ\zeta(x)/v} \frac{1}{\sqrt{2}} (v + \eta(x)), \\ \langle 0 | \eta | 0 \rangle &= \langle 0 | \zeta | 0 \rangle = 0. \end{aligned} \quad (73)$$

Thanks to the gauge symmetry, the field $\zeta(x)$ can now be eliminated (*gauged away*) by exploiting the gauge freedom to *choose the phase* of ϕ at every point of spacetime,

$$\phi(x) \mapsto e^{-iQ\zeta(x)/v} \phi(x) = \frac{1}{\sqrt{2}} (v + \eta(x)). \quad (74)$$

The resulting lagrangian is

$$\begin{aligned} \mathcal{L} = & -\frac{1}{4} F_{\mu\nu} F^{\mu\nu} + \frac{1}{2} (\partial_\mu \eta)(\partial^\mu \eta) \\ & - \lambda v^2 \eta^2 - \lambda v \eta^3 - \frac{\lambda}{4} \eta^4 + \frac{1}{4} \lambda v^4 \\ & + \frac{1}{2} (eQv)^2 A_\mu A^\mu + \frac{1}{2} (eQ)^2 A_\mu A^\mu (2v\eta + \eta^2). \end{aligned} \quad (75)$$

Observe that we obtain again the same masses $m_\eta = \sqrt{2\lambda} v$ and $M_A = |eQv|$. Of course, since the gauge has been ‘fixed’, there is no need to add a \mathcal{L}_{GF} . Actually this corresponds to choosing the so-called *unitary gauge* (R_ξ gauge with $\xi \rightarrow \infty$), in which only the physical fields appear:

$$\begin{aligned} \tilde{D}_{\mu\nu}(k) &\rightarrow \frac{i}{k^2 - M_A^2 + i\epsilon} \left(-g_{\mu\nu} + \frac{k_\mu k_\nu}{M_A^2} \right), \\ \tilde{D}(k) &\rightarrow 0. \end{aligned} \quad (76)$$

The results above are a manifestation of the *Brout-Englert-Higgs mechanism* [9-15]. The *gauge bosons* associated with the spontaneously broken generators become massive, the corresponding *would-be Goldstone bosons* are unphysical (they can be absorbed), and the remaining massive scalars (*Higgs bosons*) are physical.

The existence of Higgs bosons is the smoking gun confirming that this mechanism is responsible for the mass of the gauge bosons associated to broken symmetries. One often says that the would-be Goldstone bosons are ‘eaten up’ by the gauge bosons that ‘get fat’ by acquiring a mass. But keep in mind that the would-be Goldstone bosons only disappear completely in the unitary gauge ($\xi \rightarrow \infty$), even though they are unphysical in any gauge.

Notice also that the number of degrees of freedom (dof) of the physical spectrum remains the same. In the case of the U(1) gauge invariance we have discussed, before spontaneous symmetry breaking ($\mu^2 > 0$) there are 2 scalars and one massless gauge boson with 2 polarizations ($1 + 1 + 2 = 4$ dof). After spontaneous symmetry breaking ($\mu^2 < 0$) one of the scalars is physical but the other one is not, and the massive gauge boson has 3 polarizations ($1 + 0 + 3 = 4$ dof).

Remember that for loop calculations the ‘t Hooft-Feynman gauge (R_ξ gauge with $\xi = 1$) is more convenient because the gauge boson propagators are simpler. However, be aware that in this gauge the Goldstone bosons must be included, in internal lines only.

For completeness, let us mention that, if the gauge group is non-abelian, the (unphysical) Faddeev-Popov ghosts associated to the gauge boson of broken symmetries acquire a gauge-dependent mass. In a general R_ξ gauge the FP propagator is

$$\tilde{D}_{ab}(k) = \frac{i\delta_{ab}}{k^2 - \xi_a M_{W_a}^2 + i\epsilon}. \quad (77)$$

Finally, it is very important to underline that gauge theories with spontaneous symmetry breaking are renormalizable [16]. This means that the ultraviolet divergences appearing at loop level can be absorbed by an appropriate redefinition of the parameters and fields in the classical lagrangian. Since there are a finite number of them, they can all be fixed by the measurement of just a few observables, so these theories are predictive.

2. The standard model

2.1. Gauge group and field representations

The Standard Model (SM) [17-22] is a gauge theory based on the symmetry group:

$$\text{SU}(3)_c \otimes \text{SU}(2)_L \otimes \text{U}(1)_Y \rightarrow \text{SU}(3)_c \otimes \text{U}(1)_Q, \quad (78)$$

where the electroweak symmetry is spontaneously broken to the electromagnetic symmetry by the Brout-Englert-Higgs mechanism.

The SM particle content, in Table I, consists of three replicas (families or generations) of spin 1/2 fermions that constitute matter, a set of $8 + 3 + 1 = 12$ gauge vector bosons

TABLE I. SM particle content: 3 fermion families of 2 quarks in 3 colors and 2 leptons, 12 gauge bosons and one Higgs boson. The electric charges Q of quarks or leptons of the same family differ in one unit.

| Fermions | | I | II | III | Q | |
|--------------------|------------|--------------------|------------|------------|------------|----------------|
| spin $\frac{1}{2}$ | Quarks | f | uuu | ccc | $t\bar{t}$ | $\frac{2}{3}$ |
| | | f' | $d\bar{d}$ | $s\bar{s}$ | $b\bar{b}$ | $-\frac{1}{3}$ |
| | Leptons | f | ν_e | ν_μ | ν_τ | 0 |
| | | f' | e | μ | τ | -1 |
| Bosons | | responsible for | | | | |
| spin 1 | 8 gluons | strong interaction | | | | |
| | W^\pm, Z | weak interaction | | | | |
| | γ | em interaction | | | | |
| spin 0 | Higgs | origin of mass | | | | |

TABLE II. Gauge group representations of left-handed and right-handed fermion fields under $SU(3)_c \otimes SU(2)_L \otimes U(1)_Y$. They are the same for each family of quarks or leptons (universal). The electric charges Q are fixed by the $SU(2)_L$ weak isospin T_3 and the $U(1)_Y$ hypercharge Y . Right-handed neutrinos are sterile (singlets) and were absent in the original SM with massless neutrinos.

| Multiplets | | I | II | III |
|------------|--|---|--|--|
| Quarks | $(\mathbf{3}, \mathbf{2}, \frac{1}{6})$ | $\begin{pmatrix} u_L \\ d_L \end{pmatrix}$ | $\begin{pmatrix} c_L \\ s_L \end{pmatrix}$ | $\begin{pmatrix} t_L \\ b_L \end{pmatrix}$ |
| | $(\mathbf{3}, \mathbf{1}, \frac{2}{3})$ | u_R | c_R | t_R |
| | $(\mathbf{3}, \mathbf{1}, -\frac{1}{3})$ | d_R | s_R | b_R |
| Leptons | $(\mathbf{1}, \mathbf{2}, -\frac{1}{2})$ | $\begin{pmatrix} \nu_{eL} \\ e_L \end{pmatrix}$ | $\begin{pmatrix} \nu_{\mu L} \\ \mu_L \end{pmatrix}$ | $\begin{pmatrix} \nu_{\tau L} \\ \tau_L \end{pmatrix}$ |
| | $(\mathbf{1}, \mathbf{1}, -1)$ | e_R | μ_R | τ_R |
| | $(\mathbf{1}, \mathbf{1}, 0)$ | ν_{eR} | $\nu_{\mu R}$ | $\nu_{\tau R}$ |
| | | | | |

mediating the fundamental interactions (as many as generators of the gauge group) and one Higgs boson, remnant of the Higgs scalar field that triggers the electroweak symmetry breaking (EWSB) giving rise to the masses of elementary particles.

The SM is a chiral theory: left and right-handed components of the fermion fields lay in different representations of the gauge group, as shown in Table II. Strong and electroweak interactions can be studied separately and have very different properties. The former, specified by $SU(3)_c$, are dubbed *quantum chromodynamics* (QCD) because they are only experienced by particles with ‘color’ charges, that is quarks (color triplets) and gluons. The electroweak interactions, described by the group $SU(2)_L \otimes U(1)_Y$, affect any type (‘flavor’) of fermions depending on their weak isospin and hypercharge (*quantum flavordynamics*). Left/right-handed fermions are isospin doublets/singlets, respectively, and have also different hypercharges. The elec-

tric charges Q are associated to the only electroweak symmetry generator that remains unbroken, the sum of the $SU(2)_L$ weak isospin T_3 and the $U(1)_Y$ hypercharge Y , leading to *quantum electrodynamics* (QED).

2.2. Electroweak interactions

2.2.1. One generation of quarks or leptons

Consider two massless fermion fields $f(x)$ and $f'(x)$ with electric charges $Q_f = Q_{f'} + 1$ and assume their chiral components lay in the following $SU(2)_L \otimes U(1)_Y$ representations:

$$\Psi_1 = \begin{pmatrix} f_L \\ f'_L \end{pmatrix} \sim (\mathbf{2}, y_1),$$

$$\psi_2 = f_R \sim (\mathbf{1}, y_2), \quad \psi_3 = f'_R \sim (\mathbf{1}, y_3), \quad (79)$$

where $f_{R,L} = P_{R,L} f$ with $P_{R,L} = (1/2)(1 \pm \gamma_5)$ the chiral projectors, and likewise for $f'_{R,L}$. Their free lagrangian, invariant under global transformations, is

$$\mathcal{L}_F^0 = i\bar{\Psi}_1 \not{\partial} \Psi_1 + i\bar{\psi}_2 \not{\partial} \psi_2 + i\bar{\psi}_3 \not{\partial} \psi_3. \quad (80)$$

To make it invariant under gauge transformations,

$$\Psi_1(x) \mapsto U_L(x) e^{-iy_1 \beta(x)} \Psi_1(x),$$

$$\psi_2(x) \mapsto e^{-iy_2 \beta(x)} \psi_2(x),$$

$$\psi_3(x) \mapsto e^{-iy_3 \beta(x)} \psi_3(x), \quad (81)$$

where $U_L(x) = \exp\{-iT_i \alpha^i(x)\}$ and $T_i = \sigma_i/2$, one has to substitute the corresponding covariant derivatives,

$$D_\mu \Psi_1 = (\partial_\mu - ig\widetilde{W}_\mu + ig'y_1 B_\mu) \Psi_1, \quad \widetilde{W}_\mu \equiv \frac{\sigma_i}{2} W_\mu^i,$$

$$D_\mu \psi_2 = (\partial_\mu + ig'y_2 B_\mu) \psi_2,$$

$$D_\mu \psi_3 = (\partial_\mu + ig'y_3 B_\mu) \psi_3, \quad (82)$$

where we have introduced two couplings, g and g' , one for each group factor, and four gauge fields, $W_\mu^1(x)$, $W_\mu^2(x)$, $W_\mu^3(x)$ and $B_\mu(x)$, transforming as:ⁱⁱⁱ

$$\widetilde{W}_\mu(x) \mapsto U_L(x) \widetilde{W}_\mu(x) U_L^\dagger(x) - \frac{i}{g} (\partial_\mu U_L(x)) U_L^\dagger(x)$$

$$B_\mu(x) \mapsto B_\mu(x) + \frac{1}{g'} \partial_\mu \beta(x). \quad (83)$$

Then \mathcal{L}_F^0 is replaced by \mathcal{L}_F , which contains charge conjugation (C) and parity (P) violating interactions. Furthermore, one has to add the Yang-Mills lagrangian

$$\mathcal{L}_{\text{YM}} = -\frac{1}{4} W_{\mu\nu}^i W^{i,\mu\nu} - \frac{1}{4} B_{\mu\nu} B^{\mu\nu}, \quad (84)$$

with $W_{\mu\nu}^i = \partial_\mu W_\nu^i - \partial_\nu W_\mu^i + g\epsilon_{ijk} W_\mu^j W_\nu^k$ and $B_{\mu\nu} = \partial_\mu B_\nu - \partial_\nu B_\mu$, which includes kinetic terms for every vector field and self-interactions for the gauge fields of $SU(2)_L$, a non-abelian symmetry.

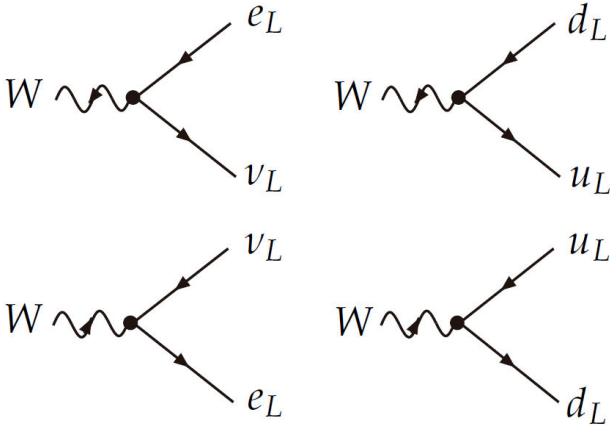


FIGURE 3. Weak charged current interactions.

Note that mass terms for the fermions are incompatible with the symmetry because left and right-handed components do not transform the same under $SU(2)_L \otimes U(1)_Y$ and

$$m\bar{f}f = m(\bar{f}_L f_R + \bar{f}_R f_L). \quad (85)$$

Mass terms for the gauge bosons are not allowed either. Both problems will be solved later. Let us discuss first the different types of interactions that have been generated.

Charged current interactions

The off-diagonal part of the term $g\bar{\Psi}_1\gamma^\mu\widetilde{W}_\mu\Psi_1$ in \mathcal{L}_F , with

$$\widetilde{W}_\mu = \frac{1}{2} \begin{pmatrix} W_\mu^3 & \sqrt{2}W_\mu^+ \\ \sqrt{2}W_\mu^- & -W_\mu^3 \end{pmatrix}, \quad (86)$$

gives rise to interactions (Fig. 3) involving f_L and f'_L and the complex weak field $W_\mu \equiv (1/\sqrt{2})(W_\mu^1 + iW_\mu^2)$,

$$\begin{aligned} \mathcal{L}_F \supset \mathcal{L}_{CC} &= \frac{g}{\sqrt{2}}\bar{f}_L\gamma^\mu f'_L W_\mu^\dagger + \text{h.c.} \\ &= \frac{g}{2\sqrt{2}}\bar{f}\gamma^\mu(1 - \gamma_5)f'W_\mu^\dagger + \text{h.c.} \end{aligned} \quad (87)$$

Note that W_μ^- , also denoted W_μ^- , annihilates W^- bosons and creates W^+ bosons, whereas W_μ^+ , also denoted W_μ^+ , does the opposite.

Neutral current interactions

The diagonal part of $g\bar{\Psi}_1\gamma^\mu\widetilde{W}_\mu\Psi_1$ and the remaining terms,

$$\begin{aligned} \mathcal{L}_F \supset \mathcal{L}_{NC} &= \frac{1}{2}g\bar{\Psi}_1\gamma^\mu\sigma_3\Psi_1 W_\mu^3 - g'(y_1\bar{\Psi}_1\gamma^\mu\Psi_1 \\ &+ y_2\bar{\psi}_2\gamma^\mu\psi_2 + y_3\bar{\psi}_3\gamma^\mu\psi_3)B_\mu, \end{aligned} \quad (88)$$

describe interactions with the vector boson fields W_μ^3 and B_μ that do not change fermion charge. We are tempted to identify B_μ with the photon field A_μ of QED but for that purpose both chiralities of each fermion should couple proportional to the fermion electric charge. However, this is not possible because it would require $y_1 = y_2 = y_3$ and $g'y_j = eQ_j$

simultaneously. Since both W_μ^3 and B_μ are neutral, one introduces the following orthogonal combinations,

$$\begin{pmatrix} W_\mu^3 \\ B_\mu \end{pmatrix} \equiv \begin{pmatrix} c_W & -s_W \\ s_W & c_W \end{pmatrix} \begin{pmatrix} Z_\mu \\ A_\mu \end{pmatrix}, \quad (89)$$

where $s_W \equiv \sin\theta_W$, $c_W \equiv \cos\theta_W$ and θ_W is the weak mixing or Weinberg angle.^{iv} Then

$$\begin{aligned} \mathcal{L}_{NC} &= \sum_{j=1}^3 \bar{\psi}_j\gamma^\mu \{ -[gT_3s_W + g'y_jc_W]A_\mu \\ &+ [gT_3c_W - g'y_js_W]Z_\mu \} \psi_j, \end{aligned} \quad (90)$$

where $T_3 = (1/2)\sigma_3$ ($T_3 = 0$) is here the third weak isospin component of the doublet (singlet), and we have introduced $\psi_1 \equiv \Psi_1$ to alleviate the notation. To make A_μ the photon field is now enough to establish the relations:

$$e = g s_W = g' c_W, \quad Q = T_3 + Y. \quad (91)$$

This is the celebrated *electroweak unification*, connecting the couplings g of $SU(2)_L$ and g' of $U(1)_Y$ to the electromagnetic coupling $e = gg'/\sqrt{g^2 + g'^2}$ of $U(1)_Q$. The electric charges of f and f' are embedded in the operators

$$Q_1 = \begin{pmatrix} Q_f & 0 \\ 0 & Q_{f'} \end{pmatrix}, \quad Q_2 = Q_f, \quad Q_3 = Q_{f'}, \quad (92)$$

so the hypercharges are given in terms of electric charges and weak isospin as shown in Table II;

$$y_1 = Q_f - \frac{1}{2} = Q_{f'} + \frac{1}{2}, \quad y_2 = Q_f, \quad y_3 = Q_{f'}. \quad (93)$$

As a consequence, $\mathcal{L}_{NC} = \mathcal{L}_{QED} + \mathcal{L}_{NC}^Z$ contains the electromagnetic interactions mediated by the photon field (Fig. 4a),

$$\mathcal{L}_{QED} = -eQ_f\bar{f}\gamma^\mu f A_\mu + (f \rightarrow f') \quad (94)$$

and weak neutral current interactions mediated by the Z boson field (Fig. 4b),

$$\mathcal{L}_{NC}^Z = e\bar{f}\gamma^\mu(v_f - a_f\gamma_5)f Z_\mu + (f \rightarrow f'), \quad (95)$$

with

$$v_f = \frac{T_3^{fL} - 2Q_f s_W^2}{2s_W c_W}, \quad a_f = \frac{T_3^{fL}}{2s_W c_W}, \quad (96)$$

where T_3^{fL} refers to the eigenvalue of T_3 that corresponds to f_L . Note that left-handed neutrinos ν_L have only weak interactions, while right-handed ν_R would be sterile, hence absent in the original SM with massless neutrinos.

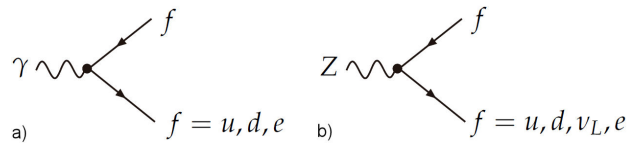


FIGURE 4. Electromagnetic and weak neutral current interactions.

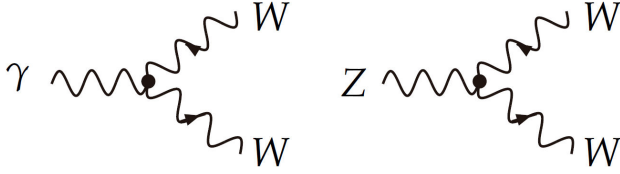


FIGURE 5. Triple gauge boson interactions.

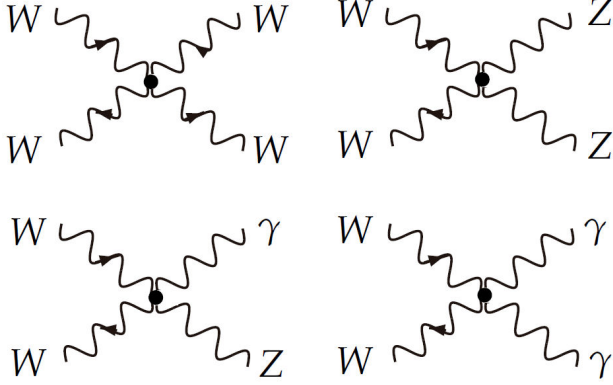


FIGURE 6. Quartic gauge boson interactions.

Gauge boson self-interactions

After some algebra, from the Yang-Mills lagrangian (84) and the field redefinitions (89), one may derive cubic interactions among the gauge boson fields (Fig. 5),

$$\begin{aligned} \mathcal{L}_{\text{YM}} \supset \mathcal{L}_3 = & -\frac{ie c_W}{s_W} \{W^{\mu\nu} W_\mu^\dagger Z_\nu - W_{\mu\nu}^\dagger W^\mu Z^\nu \\ & - W_\mu^\dagger W_\nu Z^{\mu\nu}\} + ie \{W^{\mu\nu} W_\mu^\dagger A_\nu \\ & - W_{\mu\nu}^\dagger W^\mu A^\nu - W_\mu^\dagger W_\nu F^{\mu\nu}\}, \end{aligned} \quad (97)$$

with $F_{\mu\nu} = \partial_\mu A_\nu - \partial_\nu A_\mu$, $Z_{\mu\nu} = \partial_\mu Z_\nu - \partial_\nu Z_\mu$, $W_{\mu\nu} = \partial_\mu W_\nu - \partial_\nu W_\mu$, and quartic interactions (Fig. 6),

$$\begin{aligned} \mathcal{L}_{\text{YM}} \supset \mathcal{L}_4 = & -\frac{e^2}{2s_W^2} \left\{ (W_\mu^\dagger W^\mu)^2 - W_\mu^\dagger W^\mu W_\nu^\dagger W^\nu \right\} \\ & - \frac{e^2 c_W^2}{s_W^2} \{W_\mu^\dagger W^\mu Z_\nu Z^\nu - W_\mu^\dagger Z^\mu W_\nu Z^\nu\} \\ & + \frac{e^2 c_W}{s_W} \{2W_\mu^\dagger W^\mu Z_\nu A^\nu - W_\mu^\dagger Z^\mu W_\nu A^\nu - W_\mu^\dagger A^\mu W_\nu Z^\nu\} \\ & - e^2 \{W_\mu^\dagger W^\mu A_\nu A^\nu - W_\mu^\dagger A^\mu W_\nu A^\nu\}. \end{aligned} \quad (98)$$

Note that gauge boson self-interactions involve an even number of W and there is no vertex with only γ or Z .

2.2.2. Electroweak symmetry breaking: Higgs sector and gauge boson masses

The weak gauge bosons, W^\pm and Z , are massive. To provide them with masses without explicitly breaking gauge invariance one resorts to the Higgs mechanism, that allows

to break spontaneously three out of the four generators of $\text{SU}(2)_L \otimes \text{U}(1)_Y$, T_1, T_2, T_3, Y , preserving the combination $Q = T_3 + Y$ unbroken, so that the photon remains massless.

This cannot be achieved by just introducing one complex scalar field. A complex Higgs doublet of $\text{SU}(2)$ with the appropriate hypercharge will do the work,

$$\Phi = \begin{pmatrix} \phi^+ \\ \phi^0 \end{pmatrix}, \quad \langle 0 | \Phi | 0 \rangle \equiv \frac{1}{\sqrt{2}} \begin{pmatrix} 0 \\ v \end{pmatrix}, \quad (99)$$

where $v/\sqrt{2}$ is the Higgs vacuum expectation value, minimum of the mexican hat potential $V(\Phi)$,

$$V(\Phi) = \mu^2 \Phi^\dagger \Phi + \lambda (\Phi^\dagger \Phi)^2, \quad (100)$$

and $\mu^2 = -\lambda v^2 < 0$. The Higgs lagrangian is gauge invariant thanks to the covariant derivatives, that lead to interactions with the gauge fields:

$$\begin{aligned} \mathcal{L}_\Phi &= (D_\mu \Phi)^\dagger D^\mu \Phi - V(\Phi), \\ D_\mu \Phi &= (\partial_\mu - ig \widetilde{W}_\mu + ig' y_\Phi B_\mu) \Phi. \end{aligned} \quad (101)$$

By assigning a hypercharge $y_\Phi = 1/2$ to the Higgs doublet one gets a generator that annihilates the vacuum (associated to the photon field) and three that do not (associated to the massive vector fields), as we wanted:

$$\begin{aligned} (T_3 + Y) |0\rangle &= Q \begin{pmatrix} 0 \\ v \end{pmatrix} = 0, \\ \{T_1, T_2, T_3 - Y\} |0\rangle &\neq 0. \end{aligned} \quad (102)$$

In the unitary gauge one parametrizes the three would-be-Goldstone fields in $\Phi(x)$ as spacetime-dependent phases that can be absorbed (gauged away) thanks to the gauge freedom,

$$\begin{aligned} \Phi(x) &\equiv \exp \left\{ i \frac{\sigma_i}{2v} \theta^i(x) \right\} \frac{1}{\sqrt{2}} \begin{pmatrix} 0 \\ v + H(x) \end{pmatrix} \\ &\mapsto \exp \left\{ -i \frac{\sigma_i}{2v} \theta^i(x) \right\} \Phi(x) = \frac{1}{\sqrt{2}} \begin{pmatrix} 0 \\ v + H(x) \end{pmatrix}. \end{aligned} \quad (103)$$

Only the Higgs field $H(x)$ is physical. The three degrees of freedom apparently lost become the extra (longitudinal) polarizations of W^\pm and Z that are massive particles of spin 1 after the EWSB. Replacing Eq. (103) in (101) one gets the gauge boson mass terms:

$$\begin{aligned} \mathcal{L}_\Phi \supset \mathcal{L}_M &= \frac{g^2 v^2}{4} W_\mu^\dagger W^\mu + \frac{g^2 v^2}{8c_W^2} Z_\mu Z^\mu \\ &\Rightarrow M_W = M_Z c_W = \frac{1}{2} g v. \end{aligned} \quad (104)$$

The fact that the parameter $\rho \equiv M_W^2 / (M_Z c_W)^2 = 1$ is a consequence of the custodial symmetry, a residual global $\text{SU}(2)$ symmetry of $V(\Phi)$ after EWSB when Φ is a complex Higgs doublet.^v The ρ parameter measures the relative strength of neutral-current to charged-current interactions,

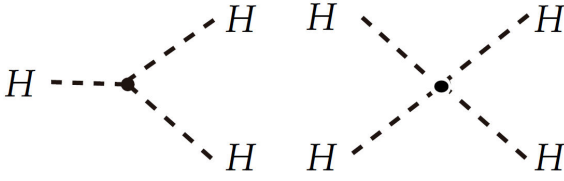


FIGURE 7. Higgs boson self-interactions.

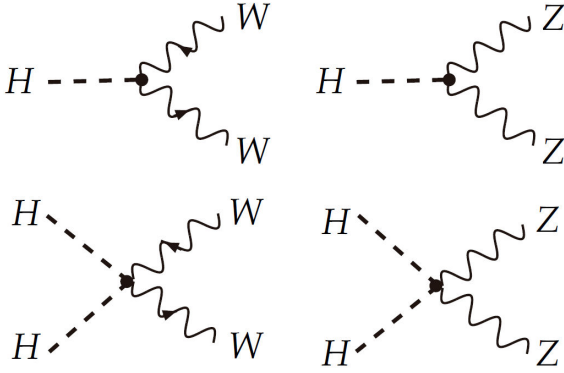


FIGURE 8. Higgs-gauge boson interactions.

but the tree-level relation $\rho = 1$ is slightly broken by quantum corrections (see *e.g.* [2]).

In the unitary gauge, where only physical fields are manifest, apart from the gauge boson mass terms, the Higgs Lagrangian contains the (physical) Higgs kinetic terms, its self-interactions (Fig. 7) and the Higgs-gauge boson interactions (Fig. 8):^{vi}

$$\mathcal{L}_\Phi = \mathcal{L}_H + \mathcal{L}_M + \mathcal{L}_{HV},$$

$$\mathcal{L}_H = \frac{1}{2} \partial_\mu H \partial^\mu H - \frac{1}{2} M_H^2 H^2 - \frac{M_H^2}{2v} H^3 - \frac{M_H^2}{8v^2} H^4,$$

$$\begin{aligned} \mathcal{L}_M + \mathcal{L}_{HV} = & M_W^2 W_\mu^\dagger W^\mu \left\{ 1 + \frac{2}{v} H + \frac{H^2}{v^2} \right\} \\ & + \frac{1}{2} M_Z^2 Z_\mu Z^\mu \left\{ 1 + \frac{2}{v} H + \frac{H^2}{v^2} \right\}, \end{aligned} \quad (105)$$

where

$$M_H = \sqrt{-2\mu^2} = \sqrt{2\lambda} v. \quad (106)$$

However, it is often more convenient to use R_ξ gauges, where the Higgs doublet is parametrized as

$$\Phi(x) \equiv \left(\frac{\phi^+(x)}{\frac{1}{\sqrt{2}}[v + H(x) + i\chi(x)]} \right), \quad (107)$$

and $\phi^-(x) \equiv [\phi^+(x)]^\dagger$. Then the Higgs Lagrangian reads

$$\begin{aligned} \mathcal{L}_\Phi = & \mathcal{L}_H + \mathcal{L}_M + \mathcal{L}_{HV^2} \\ & + (\partial_\mu \phi^+) (\partial^\mu \phi^-) + \frac{1}{2} (\partial_\mu \chi) (\partial^\mu \chi) \\ & + iM_W (W_\mu \partial^\mu \phi^+ - W_\mu^\dagger \partial^\mu \phi^-) + M_Z Z_\mu \partial^\mu \chi + \dots \end{aligned} \quad (108)$$

The omitted terms include trilinear (SSS, SSV, SVV) and quadrilinear (SSSS, SSVV) interactions of vector (V) and scalar (S) fields involving would-be-Goldstone bosons, that can be easily derived.

In order to define propagators and remove the cross terms $W_\mu \partial^\mu \phi^+$, $W_\mu^\dagger \partial^\mu \phi^-$, $Z_\mu \partial^\mu \chi$ an appropriate gauge-fixing Lagrangian must be added,

$$\begin{aligned} \mathcal{L}_{\text{GF}} = & -\frac{1}{2\xi_\gamma} (\partial_\mu A^\mu)^2 - \frac{1}{2\xi_Z} (\partial_\mu Z^\mu - \xi_Z M_Z \chi)^2 \\ & - \frac{1}{\xi_W} |\partial_\mu W^\mu + i\xi_W M_W \phi^-|^2. \end{aligned} \quad (109)$$

Then one finds a massless photon propagator, massive propagators for the weak gauge bosons and propagators for the unphysical would-be Goldstone bosons, whose masses are gauge dependent:

$$\begin{aligned} \tilde{D}_{\mu\nu}^\gamma(k) = & \frac{i}{k^2 + i\epsilon} \left[-g_{\mu\nu} + (1 - \xi_\gamma) \frac{k_\mu k_\nu}{k^2} \right], \\ \tilde{D}_{\mu\nu}^Z(k) = & \frac{i}{k^2 - M_Z^2 + i\epsilon} \left[-g_{\mu\nu} + (1 - \xi_Z) \frac{k_\mu k_\nu}{k^2 - \xi_Z M_Z^2} \right], \\ \tilde{D}_{\mu\nu}^W(k) = & \frac{i}{k^2 - M_W^2 + i\epsilon} \left[-g_{\mu\nu} + (1 - \xi_W) \frac{k_\mu k_\nu}{k^2 - \xi_W M_W^2} \right], \\ \tilde{D}^\chi(k) = & \frac{i}{k^2 - \xi_Z M_Z^2 + i\epsilon}, \\ \tilde{D}^\phi(k) = & \frac{i}{k^2 - \xi_W M_W^2 + i\epsilon}. \end{aligned} \quad (110)$$

These propagators are much simpler in the 't Hooft-Feynman gauge, where $\xi_\gamma = \xi_Z = \xi_W = 1$, which is particularly useful for loop calculations.

Last but not least, the electroweak symmetry group is non-abelian, so Faddeev-Popov ghosts must be introduced, one per SU(2) generator, in order to restore the gauge invariance of the theory at the quantum level. After the EWSB they do not only couple to the SU(2) gauge fields but also to the Higgs doublet,

$$\begin{aligned} \mathcal{L}_{\text{FP}} = & (\partial^\mu \bar{c}_i) (\partial_\mu c_i - g \epsilon_{ijk} c_j W_\mu^k) \\ & + \text{ghost interactions with } \Phi. \end{aligned} \quad (111)$$

These auxiliary fields $c_i(x)$ ($i = 1, 2, 3$) are usually written in terms of combinations associated to the ordinary weak and electromagnetic vector fields,

$$\begin{aligned} c_1 \equiv & \frac{1}{\sqrt{2}}(u_+ + u_-), \quad c_2 \equiv \frac{i}{\sqrt{2}}(u_+ - u_-), \\ c_3 \equiv & c_W u_Z - s_W u_\gamma. \end{aligned} \quad (112)$$

For completeness, the full expression of the Faddeev-Popov Lagrangian is as follows:

$$\begin{aligned}
\mathcal{L}_{\text{FP}} = & (\partial_\mu \bar{u}_\gamma)(\partial^\mu u_\gamma) + (\partial_\mu \bar{u}_Z)(\partial^\mu u_Z) + (\partial_\mu \bar{u}_+) (\partial^\mu u_+) + (\partial_\mu \bar{u}_-) (\partial^\mu u_-) + ie[(\partial^\mu \bar{u}_+)u_+ - (\partial^\mu \bar{u}_-)u_-]A_\mu \\
& - \frac{ie c_W}{s_W} [(\partial^\mu \bar{u}_+)u_+ - (\partial^\mu \bar{u}_-)u_-]Z_\mu - ie[(\partial^\mu \bar{u}_+)u_\gamma - (\partial^\mu \bar{u}_\gamma)u_-]W_\mu^\dagger + \frac{ie c_W}{s_W} [(\partial^\mu \bar{u}_+)u_Z - (\partial^\mu \bar{u}_Z)u_-]W_\mu^\dagger \\
& + ie[(\partial^\mu \bar{u}_-)u_\gamma - (\partial^\mu \bar{u}_\gamma)u_+]W_\mu - \frac{ie c_W}{s_W} [(\partial^\mu \bar{u}_-)u_Z - (\partial^\mu \bar{u}_Z)u_+]W_\mu - \xi_Z M_Z^2 \bar{u}_Z u_Z - \xi_W M_W^2 \bar{u}_+ u_+ \\
& - \xi_W M_W^2 \bar{u}_- u_- - e \xi_Z M_Z \bar{u}_Z \left[\frac{1}{2s_W c_W} H u_Z - \frac{1}{2s_W} (\phi^+ u_- + \phi^- u_+) \right] \\
& - e \xi_W M_W \bar{u}_+ \left[\frac{1}{2s_W} (H + i\chi) u_+ - \phi^+ \left(u_\gamma - \frac{c_W^2 - s_W^2}{2s_W c_W} u_Z \right) \right] \\
& - e \xi_W M_W \bar{u}_- \left[\frac{1}{2s_W} (H - i\chi) u_- - \phi^- \left(u_\gamma - \frac{c_W^2 - s_W^2}{2s_W c_W} u_Z \right) \right]. \tag{113}
\end{aligned}$$

From the kinetic terms one can directly see that ghost propagators contain gauge-dependent masses that coincide with those of the partner gauge boson fields in the 't Hooft-Feynman gauge,

$$\begin{aligned}
\tilde{D}^{u_\gamma}(k) &= \frac{i}{k^2 + i\epsilon}, \quad \tilde{D}^{u_Z}(k) = \frac{i}{k^2 - \xi_Z M_Z^2 + i\epsilon}, \\
\tilde{D}^{u_\pm}(k) &= \frac{i}{k^2 - \xi_W M_W^2 + i\epsilon}. \tag{114}
\end{aligned}$$

The interaction terms include trilinear (UUV) and quadrilinear (SUU) interactions of vector (V) and unphysical ghost fields (U).

2.2.3. Yukawa interactions: fermion masses

Masses for quarks and leptons are also needed, without spoiling the gauge symmetry. For that purpose *another* interaction is introduced that couples the Higgs doublet Φ to the fermion fields preserving the $SU(2)_L \otimes U(1)_Y$ symmetry. Since the left-handed components make a doublet and the right-handed ones are singlets, this can be achieved with the following Yukawa interactions:

$$\begin{aligned}
\mathcal{L}_Y = & -\lambda_d (\bar{u}_L \bar{d}_L) \Phi d_R - \lambda_u (\bar{u}_L \bar{d}_L) \tilde{\Phi} u_R \\
& - \lambda_e (\bar{\nu}_L \bar{e}_L) \Phi e_R - \lambda_\nu (\bar{\nu}_L \bar{e}_L) \tilde{\Phi} \nu_R + \text{h.c.}, \tag{115}
\end{aligned}$$

where $\tilde{\Phi} \equiv i\sigma_2 \Phi^*$ has the appropriate quantum numbers for interactions involving up-type fermion singlets. The neutrino Yukawa coupling was not introduced in the original SM with massless neutrinos, but we keep it for further reference. After the EWSB, fermions acquire masses proportional to the corresponding Yukawa couplings,

$$\begin{aligned}
\mathcal{L}_Y \supset & -\frac{1}{\sqrt{2}}(v + H) \{ \lambda_d \bar{d}d + \lambda_u \bar{u}u + \lambda_e \bar{e}e + \lambda_\nu \bar{\nu}\nu \} \\
\Rightarrow & m_f = \lambda_f \frac{v}{\sqrt{2}}, \tag{116}
\end{aligned}$$

recalling that $\bar{f}f = \bar{f}_L f_R + \bar{f}_R f_L$.

2.2.4. Additional generations: fermion mixings

We know of 3 generations of quarks and leptons in nature. They are identical copies with the same properties under $SU(2)_L \otimes U(1)_Y$ differing only in their masses. If one takes n generations and defines $u_i^I, d_i^I, \nu_i^I, e_i^I$ as the fields corresponding to the i -th generation, where the superindex I (standing for 'interaction' basis) was omitted so far, the most general gauge-invariant Yukawa lagrangian is

$$\begin{aligned}
\mathcal{L}_Y = & - \sum_{ij} \left\{ \left(\bar{u}_{iL}^I \bar{d}_{iL}^I \right) \Phi \lambda_{ij}^{(d)} d_{jR}^I \right. \\
& + \left(\bar{u}_{iL}^I \bar{d}_{iL}^I \right) \tilde{\Phi} \lambda_{ij}^{(u)} u_{jR}^I \\
& + \left(\bar{\nu}_{iL}^I \bar{e}_{iL}^I \right) \Phi \lambda_{ij}^{(e)} e_{jR}^I \\
& \left. + \left(\bar{\nu}_{iL}^I \bar{e}_{iL}^I \right) \tilde{\Phi} \lambda_{ij}^{(\nu)} \nu_{jR}^I \right\} + \text{h.c.} \tag{117}
\end{aligned}$$

Here, $\lambda_{ij}^{(d)}, \lambda_{ij}^{(u)}, \lambda_{ij}^{(e)}$ (and $\lambda_{ij}^{(\nu)}$ if present) are $n \times n$ Yukawa matrices in flavor space. After EWSB this lagrangian contains the following terms in n -dimensional matrix form:

$$\begin{aligned}
\mathcal{L}_Y \supset & - \left(1 + \frac{H}{v} \right) \left\{ \bar{\mathbf{d}}_L^I \mathbf{M}_d \mathbf{d}_R^I + \bar{\mathbf{u}}_L^I \mathbf{M}_u \mathbf{u}_R^I \right. \\
& \left. + \bar{\mathbf{e}}_L^I \mathbf{M}_e \mathbf{e}_R^I + \bar{\mathbf{\nu}}_L^I \mathbf{M}_\nu \mathbf{\nu}_R^I + \text{h.c.} \right\}, \tag{118}
\end{aligned}$$

where the various mass matrices have the form $(\mathbf{M}_f)_{ij} = \lambda_{ij}^{(f)} v / \sqrt{2}$. Their diagonalization determines the (physical) mass eigenfields d_j, u_j, e_j, ν_j in terms of interaction eigenfields $d_j^I, u_j^I, e_j^I, \nu_j^I$, respectively, the latter having well-defined flavor. Each \mathbf{M}_f can be written as

$$\begin{aligned}
\mathbf{M}_f &= \mathbf{H}_f \mathcal{U}_f = \mathbf{V}_f^\dagger \mathcal{M}_f \mathbf{V}_f \mathcal{U}_f \\
\Leftrightarrow \mathbf{M}_f \mathbf{M}_f^\dagger &= \mathbf{H}_f^2 = \mathbf{V}_f^\dagger \mathcal{M}_f^2 \mathbf{V}_f, \tag{119}
\end{aligned}$$

with $\mathbf{H}_f \equiv \sqrt{\mathbf{M}_f \mathbf{M}_f^\dagger}$ a hermitian positive definite matrix and \mathcal{U}_f unitary. \mathbf{H}_f can be diagonalized by a unitary matrix \mathbf{V}_f and the resulting \mathcal{M}_f is diagonal and positive definite. In the physical basis, where mass matrices are diagonal, $\mathcal{M}_d = \text{diag}(m_d, m_s, m_b, \dots)$, $\mathcal{M}_u = \text{diag}(m_u, m_c, m_t, \dots)$, $\mathcal{M}_e = \text{diag}(m_e, m_\mu, m_\tau, \dots)$, $\mathcal{M}_\nu = \text{diag}(m_{\nu_e}, m_{\nu_\mu}, m_{\nu_\tau}, \dots)$, one finds that fermion couplings to the Higgs are proportional to fermion masses,

$$\mathcal{L}_Y \supset - \left(1 + \frac{H}{v}\right) \{ \bar{\mathbf{d}} \mathcal{M}_d \mathbf{d} + \bar{\mathbf{u}} \mathcal{M}_u \mathbf{u} + \bar{\mathbf{e}} \mathcal{M}_e \mathbf{e} + \bar{\nu} \mathcal{M}_\nu \nu \}. \quad (120)$$

Replacing now interaction with mass eigenfields,

$$\begin{aligned} \mathbf{d}_L &\equiv \mathbf{V}_d \mathbf{d}_L^I, & \mathbf{u}_L &\equiv \mathbf{V}_u \mathbf{u}_L^I, \\ \mathbf{e}_L &\equiv \mathbf{V}_e \mathbf{e}_L^I, & \nu_L &\equiv \mathbf{V}_\nu \nu_L^I, \\ \mathbf{d}_R &\equiv \mathbf{V}_d \mathcal{M}_d \mathbf{d}_R^I, & \mathbf{u}_R &\equiv \mathbf{V}_u \mathcal{M}_u \mathbf{u}_R^I, \\ \mathbf{e}_R &\equiv \mathbf{V}_e \mathcal{M}_e \mathbf{e}_R^I, & \nu_R &\equiv \mathbf{V}_\nu \mathcal{M}_\nu \nu_R^I, \end{aligned} \quad (121)$$

it is apparent that neutral-current interactions will keep the same form, because $\bar{\mathbf{f}}_L^I \mathbf{f}_L^I = \bar{\mathbf{f}}_L \mathbf{f}_L$ and $\bar{\mathbf{f}}_R^I \mathbf{f}_R^I = \bar{\mathbf{f}}_R \mathbf{f}_R$, implying that there are no flavor changing neutral currents (FCNC) at tree level. However, the operators involved in charged current interaction terms are not necessarily diagonal in the basis of mass eigenfields. For instance, in the quark sector,

$$\bar{\mathbf{u}}_L^I \mathbf{d}_L^I = \bar{\mathbf{u}}_L \mathbf{V}_u \mathbf{V}_d^\dagger \mathbf{d}_L = \bar{\mathbf{u}}_L \mathbf{V} \mathbf{d}_L. \quad (122)$$

The unitary matrix $\mathbf{V} \equiv \mathbf{V}_u \mathbf{V}_d^\dagger$ is the Cabibbo-Kobayashi-Maskawa (CKM) mixing matrix [23, 24] accounting for quark flavor misalignment and inducing inter-family transitions (Fig. 9),

$$\begin{aligned} \mathcal{L}_{CC} &= \frac{g}{\sqrt{2}} \sum_{ij} \bar{u}_L^i \gamma^\mu \mathbf{V}_{ij} d_{Lj} W_\mu^\dagger + \text{h.c.} \\ &= \frac{g}{2\sqrt{2}} \sum_{ij} \bar{u}_i \gamma^\mu (1 - \gamma_5) \mathbf{V}_{ij} d_j W_\mu^\dagger + \text{h.c.} \end{aligned} \quad (123)$$

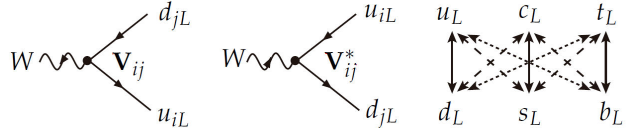


FIGURE 9. Weak charged currents change quark family proportionally to the CKM matrix elements \mathbf{V}_{ij} .

Thanks to these flavor changes in charged currents, FCNC will appear at the loop level but they are then suppressed (GIM mechanism [25]).

Note that if u_i or d_j had degenerate masses, which is not the case, one could choose $\mathbf{V}_u = \mathbf{V}_d$ by field redefinitions and quark families would not mix. Masses and mixings are observable, but the matrix elements of \mathbf{V}_u and \mathbf{V}_d are not.

Applying the same reasoning, in a lepton sector with massless neutrinos there is no lepton mixing.

At this point, it is important to discuss how many of the mixing parameters we have introduced are physical. The number of real parameters of a general $n \times n$ unitary matrix, like the CKM, is $n^2 = n(n-1)/2$ moduli + $n(n+1)/2$ phases. However, some phases are unphysical since they can be absorbed by field phase-redefinitions,

$$\begin{aligned} u_i &\rightarrow e^{i\alpha_i} u_i, \\ d_j &\rightarrow e^{i\beta_j} d_j \Rightarrow \mathbf{V}_{ij} \rightarrow \mathbf{V}_{ij} e^{-i(\alpha_i - \beta_j)}. \end{aligned} \quad (124)$$

Therefore, after removing $2n-1$ phases, the number of physical parameters is $(n-1)^2 = n(n-1)/2$ moduli + $(n-1)(n-2)/2$ phases. In particular, for the case of $n=2$ generations, there is only 1 parameter, the Cabibbo angle θ_C :

$$\mathbf{V} = \begin{pmatrix} \cos \theta_C & \sin \theta_C \\ -\sin \theta_C & \cos \theta_C \end{pmatrix}. \quad (125)$$

For the actual case of $n=3$ generations, there are 3 angles and 1 phase. In the so-called standard parametrization,

$$\begin{aligned} \mathbf{V} &= \begin{pmatrix} \mathbf{V}_{ud} & \mathbf{V}_{us} & \mathbf{V}_{ub} \\ \mathbf{V}_{cd} & \mathbf{V}_{cs} & \mathbf{V}_{cb} \\ \mathbf{V}_{td} & \mathbf{V}_{ts} & \mathbf{V}_{tb} \end{pmatrix} = \begin{pmatrix} 1 & 0 & 0 \\ 0 & c_{23} & s_{23} \\ 0 & -s_{23} & c_{23} \end{pmatrix} \begin{pmatrix} c_{13} & 0 & s_{13} e^{-i\delta} \\ 0 & 1 & 0 \\ -s_{13} e^{i\delta} & 0 & c_{13} \end{pmatrix} \begin{pmatrix} c_{12} & s_{12} & 0 \\ -s_{12} & c_{12} & 0 \\ 0 & 0 & 1 \end{pmatrix} \\ &= \begin{pmatrix} c_{12} c_{13} & s_{12} c_{13} & s_{13} e^{-i\delta} \\ -s_{12} c_{23} - c_{12} s_{23} s_{13} e^{i\delta} & c_{12} c_{23} - s_{12} s_{23} s_{13} e^{i\delta} & s_{23} c_{13} \\ s_{12} s_{23} - c_{12} c_{23} s_{13} e^{i\delta} & -c_{12} s_{23} - s_{12} c_{23} s_{13} e^{i\delta} & c_{23} c_{13} \end{pmatrix}, \end{aligned} \quad (126)$$

with $c_{ij} \equiv \cos \theta_{ij} \geq 0$, $s_{ij} \equiv \sin \theta_{ij} \geq 0$ ($i < j = 1, 2, 3$) and $0 \leq \delta \leq 2\pi$. The complex phase δ is the only source of CP violation in the SM lagrangian, requiring the existence of at least three generations of quarks. Since quarks are confined in hadrons by the strong interaction, the values of the CKM parameters are obtained from a variety of hadronic weak decays [26],

$$\theta_{12} \equiv \theta_C \approx 13^\circ, \quad \theta_{23} \approx 2.3^\circ, \quad \theta_{13} \approx 0.2^\circ, \quad \delta \approx 68^\circ. \quad (127)$$

Interestingly, any CP-violating observable must be proportional to the Jarlskog invariant [27] given by $\text{Im}(V_{ij} V_{kl} V_{il}^* V_{kj}^*) = J \sum_{m,n} \epsilon_{ikm} \epsilon_{jln}$ (phase-convention independent). In the standard parametrization $J = c_{12} c_{23} c_{13}^2 s_{12} s_{23} s_{13} \sin \delta$. The empiri-

cal value of $J \approx 3 \times 10^{-5}$ is small compared with its mathematical maximum of $1/(6\sqrt{3}) \approx 0.1$, showing that CP violation is suppressed in the quark sector.

As already mentioned, if neutrinos were massless there would be no lepton mixing. However, the observed phenomenon of neutrino oscillation requires that neutrinos have non-degenerate masses (though very light) and mix. A possible minimal extension of the original SM consists of introducing gauge-singlet neutrinos ν_R with just Yukawa couplings to the Higgs and the lepton doublet, like the other fermions, as was suggested in Eqs. (115) and (117). This ν SM [28] is however not very satisfactory: in order to get neutrino masses $m_\nu \lesssim 0.1$ eV one needs tiny Yukawa couplings $\lambda_\nu = \sqrt{2}m_\nu/v \lesssim 10^{-12}$, which apart from being unnatural would predict untestable phenomenology. Alternatively, one can exploit that neutrinos are *special* because, in contrast to the other fermions, neutrinos *may* be their own antiparticle (Majorana fermions). Then neutrinos can have gauge invariant (but lepton number violating) Majorana mass terms (m_R), in addition to the usual Dirac mass terms (m_D) from Yukawa interactions with the Higgs doublet, opening the possibility of new mechanisms for the generation of masses and mixings. Particularly interesting is the type-I seesaw mechanism [29, 30] that explains why the active neutrinos are so light by introducing gauge singlets N_R with very large Majorana mass terms $m_R \gtrsim 10^{14}$ GeV and Dirac masses $m_D \sim v/\sqrt{2} \sim 100$ GeV: the resulting mass eigenstates comprise light Majorana neutrinos that are very approximately $\nu = \nu_L + \nu_L^c$, of masses $m_\nu \approx m_D^2/m_R$, and super heavy ones, nearly $N = N_R^c + N_R$, of masses $m_N \approx m_R$, with negligible light-heavy mixings of order $m_D/m_R \sim \sqrt{m_\nu/m_N}$. Majorana fields are self-conjugate ($\nu = \nu^c$), so their chiral components are related. Furthermore, if neutrinos are Majorana particles resulting from the admixture of active and singlet neutrinos, only the active components would experience charged current interactions, and there would be FCNC at tree level in the neutrino sector involving both chiral components (see for instance Ref. [31]). As a consequence the intergenerational lepton mixings include additional CP phases that now cannot be absorbed because it is no longer possible to perform neutrino field phase-redefinitions. In any case, global fits to neutrino oscillations are compatible with 3 generations of active neutrino flavors $\nu_{\alpha L}$ ($\alpha = e, \mu, \tau$) that are an admixture of 3 light neutrino mass-eigenstates ν_{iL} ($i = 1, 2, 3$),

$$\nu_{\alpha L} = \sum_i \mathbf{U}_{\alpha i} \nu_{iL}, \quad (128)$$

where the Pontecorvo-Maki-Nakagawa-Sakata (PMNS) matrix \mathbf{U} [32–34] is the unitary mixing matrix \mathbf{V}_ν^\dagger in Eq. (121), or perhaps, if neutrinos are Majorana particles, the nearly unitary 3×3 block of a larger unitary matrix diagonalizing the Majorana neutrino mass matrix that includes both light and heavy species.

The oscillation phenomenon occurs because the mass differences among the various light mass eigenstates are so small that the *coherent superposition* ν_α in Eq. (128) can be produced or detected in a charged current interaction with the corresponding lepton e_α (e, μ, τ), as in Fig. 10. Then the probability that a (relativistic) neutrino in a quantum state of flavor α is detected as a flavor β after traveling (in vacuum) a distance $L = t$ is given by (see Fig. 11)

$$\begin{aligned} |\nu_\alpha; t\rangle &= \sum_i \mathbf{U}_{\alpha i} e^{-iE_i t} |\nu_i\rangle, \quad E_i \approx E + \frac{m_i^2}{2E} \\ &\Rightarrow \langle \nu_\beta | \nu_\alpha; t \rangle = \sum_i \mathbf{U}_{\beta i}^* \mathbf{U}_{\alpha i} e^{-iE_i t} \\ &\Rightarrow P(\nu_\alpha \rightarrow \nu_\beta; L) = |\langle \nu_\beta | \nu_\alpha; L \rangle|^2 \\ &= \sum_{ij} \mathbf{U}_{\beta i}^* \mathbf{U}_{\alpha i} \mathbf{U}_{\beta j} \mathbf{U}_{\alpha j} \exp\left(-i \frac{\Delta m_{ij}^2}{2E} L\right), \quad (129) \end{aligned}$$

where $E \approx p$ is the momentum of the relativistic neutrino of mass m_i and $\Delta m_{ij}^2 \equiv m_i^2 - m_j^2$. Charged lepton flavors do not oscillate because $|\Delta m_{ij}^2| \ll \Delta m_{\mu e}^2$ [35], so they can be taken as mass eigenstates.

In the standard parametrization, the PMNS matrix reads

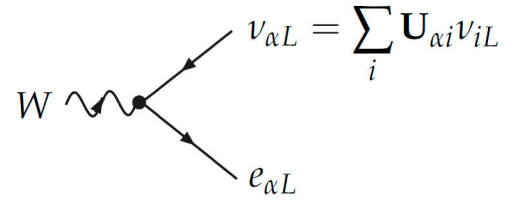
$$\nu_{\alpha L} = \sum_i \mathbf{U}_{\alpha i} \nu_{iL}$$


FIGURE 10. A neutrino flavor eigenstate ν_α , produced/detected together with a charged lepton e_α , is a coherent superposition of mass eigenstates ν_i , hence the flavor oscillates as it propagates.

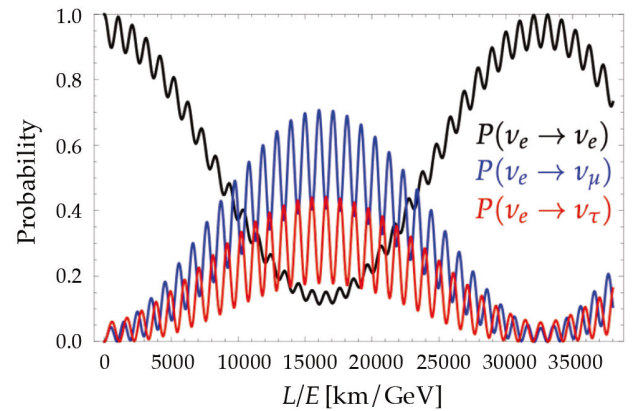


FIGURE 11. Vacuum oscillation probabilities for an initial ν_e using experimental inputs (131).

$$\mathbf{U} = \begin{pmatrix} \mathbf{U}_{e1} & \mathbf{U}_{e2} & \mathbf{U}_{e3} \\ \mathbf{U}_{\mu1} & \mathbf{U}_{\mu2} & \mathbf{U}_{\mu3} \\ \mathbf{U}_{\tau1} & \mathbf{U}_{\tau2} & \mathbf{U}_{\tau3} \end{pmatrix} = \begin{pmatrix} c_{12}c_{13} & s_{12}c_{13} & s_{13}e^{-i\delta} \\ -s_{12}c_{23} - c_{12}s_{23}s_{13}e^{i\delta} & c_{12}c_{23} - s_{12}s_{23}s_{13}e^{i\delta} & s_{23}c_{13} \\ s_{12}s_{23} - c_{12}c_{23}s_{13}e^{i\delta} & -c_{12}s_{23} - s_{12}c_{23}s_{13}e^{i\delta} & c_{23}c_{13} \end{pmatrix} \begin{pmatrix} 1 & 0 & 0 \\ 0 & e^{i\alpha_{21}/2} & 0 \\ 0 & 0 & e^{i\alpha_{31}/2} \end{pmatrix}, \quad (130)$$

where additional phases α_{21} , α_{31} are needed if neutrinos are Majorana particles, as mentioned above, and the rest are analogous to the CKM mixing parameters, though they have different values. Neutrino mass differences and mixing parameters are constrained by a good number of oscillation experiments using solar, atmospheric, accelerator and reactor neutrinos [36],

$$\Delta m_{21}^2 \approx 7.5 \times 10^{-5} \text{ eV}^2, \quad |\Delta m_{31}^2| \approx 2.5 \times 10^{-3} \text{ eV}^2 \\ \theta_{12} \equiv \theta_{\odot} \approx 34^\circ, \quad \theta_{23} \equiv \theta_{\text{atm}} \approx 49^\circ, \quad \theta_{13} \approx 8^\circ. \quad (131)$$

The best fit value of the Dirac phase δ depends on the sign of Δm_{31}^2 , that is whether the ordering of neutrino masses is normal (NO) or inverted (IO). Currently a CP-conserving value $\delta \approx 180^\circ$ is favored by NO but an almost maximal CP-violating $\delta \approx 280^\circ$ is favored by IO. Note that oscillations are not sensitive to Majorana phases as is apparent from Eq. (129). A type of experiments that can elucidate whether neutrinos are Dirac or Majorana fermions would be the observation of neutrinoless double-beta decays [37].

2.3. Electroweak phenomenology

2.3.1. Feynman rules for all vertices

The full lagrangian of the electroweak SM is

$$\mathcal{L}_{\text{EW}} = \mathcal{L}_F + \mathcal{L}_{\text{YM}} + \mathcal{L}_\Phi + \mathcal{L}_Y + \mathcal{L}_{\text{GF}} + \mathcal{L}_{\text{FP}}. \quad (132)$$

It provides a number of interactions for fermions (F), vector bosons (V) and scalar particles (S), including the physical Higgs and unphysical, would-be Goldstone bosons. And it also involves unphysical Faddeev-Popov ghost fields (U) that are auxiliary, anticommuting scalar fields. All these interactions can be cast into the following set of Lorentz-invariant lagrangians, written for convenience in terms of generic couplings normalized to appropriate powers of the electromagnetic coupling e ,

$$\begin{aligned} \mathcal{L}_{\text{FFV}} &= e \bar{\psi}_i \gamma^\mu (g_V - g_A \gamma_5) \psi_j V_\mu \\ &= e \bar{\psi}_i \gamma^\mu (g_L P_L + g_R P_R) \psi_j V_\mu, \\ \mathcal{L}_{\text{FFS}} &= e \bar{\psi}_i \gamma^\mu (g_S - g_P \gamma_5) \psi_j \phi \\ &= e \bar{\psi}_i (c_L P_L + c_R P_R) \psi_j \phi \end{aligned}$$

$$\begin{aligned} \mathcal{L}_{\text{VVV}} &= -ie c_{\text{VVV}} \\ &\times (W^{\mu\nu} W_\mu^\dagger V_\nu - W_{\mu\nu}^\dagger W^\mu V^\nu - W_\mu^\dagger W_\nu V^{\mu\nu}), \\ \mathcal{L}_{\text{VVVV}} &= e^2 c_{\text{VVVV}} \\ &\times (2W_\mu^\dagger W^\mu V_\nu V^{\nu\mu} - W_\mu^\dagger V^\mu W_\nu V^{\nu\mu} - W_\mu^\dagger V^{\nu\mu} W_\nu V^\nu), \\ \mathcal{L}_{\text{SSV}} &= -ie c_{\text{SSV}} \phi \overleftrightarrow{\partial}_\mu \phi' V^\mu, \\ \mathcal{L}_{\text{SVV}} &= e c_{\text{SVV}} \phi V^\mu V'_\mu, \\ \mathcal{L}_{\text{SSVV}} &= e^2 c_{\text{SSVV}} \phi \phi' V^\mu V'_\mu, \\ \mathcal{L}_{\text{SSS}} &= e c_{\text{SSS}} \phi \phi' \phi'', \\ \mathcal{L}_{\text{SSSS}} &= e^2 c_{\text{SSSS}} \phi \phi' \phi'' \phi''', \end{aligned} \quad (133)$$

where $g_{L,R} = g_V \pm g_A$, $c_{L,R} = g_S \pm g_P$, $\phi \overleftrightarrow{\partial}_\mu \phi' \equiv \phi \partial_\mu \phi' - (\partial_\mu \phi) \phi'$ and $V_\mu \in \{A_\mu, Z_\mu, W_\mu, W_\mu^\dagger\}$. Applying the general Feynman rules for the computation of Green functions or scattering amplitudes, the different types of interaction vertices read (momenta are taken incoming):

$$\begin{aligned} [\text{FFV}_\mu] &= ie \gamma^\mu (g_L P_L + g_R P_R), \\ [\text{FFS}] &= ie (c_L P_L + c_R P_R), \\ [\text{V}_\mu(k_1) \text{V}_\nu(k_2) \text{V}_\rho(k_3)] &= ie c_{\text{VVV}} [g_{\mu\nu}(k_2 - k_1)_\rho \\ &\quad + g_{\nu\rho}(k_3 - k_2)_\mu + g_{\mu\rho}(k_1 - k_3)_\nu], \\ [\text{V}_\mu \text{V}_\nu \text{V}_\rho \text{V}_\sigma] &= ie^2 c_{\text{VVVV}} [2g_{\mu\nu} g_{\rho\sigma} \\ &\quad - g_{\mu\rho} g_{\nu\sigma} - g_{\mu\sigma} g_{\nu\rho}], \\ [\text{S}(p) \text{S}(p') \text{V}_\mu] &= ie c_{\text{SSV}} (p_\mu - p'_\mu), \\ [\text{SV}_\mu \text{V}_\nu] &= ie c_{\text{SVV}} g_{\mu\nu}, \\ [\text{SSV}_\mu \text{V}_\nu] &= ie^2 c_{\text{SSVV}} g_{\mu\nu}, \\ [\text{SSS}] &= ie c_{\text{SSS}}, \\ [\text{SSSS}] &= ie^2 c_{\text{SSSS}}. \end{aligned} \quad (134)$$

The interactions for $[\text{UUV}_\mu \text{V}_\nu]$ and $[\text{SUU}]$ are analogous to those of $[\text{SSV}_\mu \text{V}_\nu]$ and $[\text{SSS}]$, respectively. Tables III, IV, V, VI and VII collect the values of all these generic couplings in the electroweak SM, with massless neutrinos. The couplings for would-be Goldstone bosons and Faddeev-Popov ghosts in $[\text{SSVV}]$, $[\text{SSS}]$, $[\text{SUUU}]$, $[\text{SSSS}]$ and $[\text{UUVV}]$ are omitted. All vertices can be generated by the computer package *FeynArts* [38], that uses the same sign conventions.

TABLE III. Fermion-vector boson vertices. Here $g_{\pm}^f = v_f \pm a_f$ with $v_f = (T_3^{fL} - 2Q_f s_W^2)/(2s_W c_W)$ and $a_f = T_3^{fL}/2s_W c_W$.

| FFV | $\bar{f}_i f_j \gamma$ | $\bar{f}_i f_j Z$ | $\bar{u}_i d_j W^+$ | $\bar{\nu}_i e_j W^+$ |
|-------|------------------------|---------------------|---|-------------------------------------|
| g_L | $-Q_{f_i} \delta_{ij}$ | $g_+^f \delta_{ij}$ | $\frac{1}{\sqrt{2}s_W} \mathbf{V}_{ij}$ | $\frac{1}{\sqrt{2}s_W} \delta_{ij}$ |
| g_R | $-Q_{f_i} \delta_{ij}$ | $g_-^f \delta_{ij}$ | 0 | 0 |

TABLE IV. Fermion-scalar vertices.

| FFS | $\bar{f}_i f_j H$ | $\bar{f}_i f_j \chi$ | $\bar{u}_i d_j \phi^+$ |
|-------|---|--|--|
| c_L | $-\frac{1}{2s_W} \frac{m_{f_i}}{M_W} \delta_{ij}$ | $-\frac{iT_3^{fL}}{s_W} \frac{m_{f_i}}{M_W} \delta_{ij}$ | $+\frac{1}{\sqrt{2}s_W} \frac{m_{u_i}}{M_W} \mathbf{V}_{ij}$ |
| c_R | $-\frac{1}{2s_W} \frac{m_{f_i}}{M_W} \delta_{ij}$ | $+\frac{iT_3^{fL}}{s_W} \frac{m_{f_i}}{M_W} \delta_{ij}$ | $-\frac{1}{\sqrt{2}s_W} \frac{m_{d_j}}{M_W} \mathbf{V}_{ij}^*$ |

| FFS | $\bar{\nu}_i e_j \phi^+$ | $\bar{e}_j \nu_i \phi^-$ |
|-------|--|--|
| c_L | 0 | $-\frac{1}{\sqrt{2}s_W} \frac{m_{e_j}}{M_W} \delta_{ij}$ |
| c_R | $-\frac{1}{\sqrt{2}s_W} \frac{m_{e_j}}{M_W} \delta_{ij}$ | 0 |

TABLE V. Gauge boson self-interaction vertices.

| VVV | $W^+ W^- \gamma$ | $W^+ W^- Z$ |
|-----------|------------------|-------------------|
| c_{VVV} | -1 | $\frac{c_W}{s_W}$ |

| VVVV | $W^+ W^+ W^- W^-$ | $W^+ W^- Z Z$ |
|------------|-------------------|------------------------|
| c_{VVVV} | $\frac{1}{s_W^2}$ | $-\frac{c_W^2}{s_W^2}$ |

| VVVV | $W^+ W^- \gamma Z$ | $W^+ W^- \gamma \gamma$ |
|------------|--------------------|-------------------------|
| c_{VVVV} | $\frac{c_W}{s_W}$ | -1 |

TABLE VI. Scalar-vector boson vertices.

| SSV | $\chi H Z$ | $\phi^{\pm} \phi^{\mp} \gamma$ | $\phi^{\pm} \phi^{\mp} Z$ |
|-----------|-----------------------|--------------------------------|--------------------------------------|
| c_{SSV} | $-\frac{i}{2s_W c_W}$ | ∓ 1 | $\pm \frac{c_W^2 - s_W^2}{2s_W c_W}$ |

| SSV | $\phi^{\mp} H W^{\pm}$ | $\phi^{\mp} \chi W^{\pm}$ |
|-----------|------------------------|---------------------------|
| c_{SSV} | $\mp \frac{1}{2s_W}$ | $-\frac{i}{2s_W}$ |

| SSV | $\phi^{\mp} H W^{\pm}$ | $\phi^{\mp} \chi W^{\pm}$ |
|-----------|------------------------|---------------------------|
| c_{SSV} | $\mp \frac{1}{2s_W}$ | $-\frac{i}{2s_W}$ |

| SVV | $H Z Z$ | $H W^+ W^-$ | $\phi^{\pm} W^{\mp} \gamma$ | $\phi^{\pm} W^{\mp} Z$ |
|-----------|-------------------------|-------------------|-----------------------------|------------------------|
| c_{SVV} | $\frac{M_W}{s_W c_W^2}$ | $\frac{M_W}{s_W}$ | $-M_W$ | $-\frac{M_W s_W}{c_W}$ |

| SSVV | $H H W^+ W^-$ | $H H Z Z$ |
|------------|--------------------|--------------------------|
| c_{SSVV} | $\frac{1}{2s_W^2}$ | $\frac{1}{2s_W^2 c_W^2}$ |

TABLE VII. Scalar-vector boson vertices.

| SSS | HHH | SSSS | $HHHH$ |
|-----------|----------------------------|------------|--------------------------------|
| c_{SSS} | $-\frac{3M_H^2}{2M_W s_W}$ | c_{SSSS} | $-\frac{3M_H^2}{4M_W^2 s_W^2}$ |

2.3.2. Input parameters

The electroweak gauge group introduces two couplings, $g = es_W$ and $g' = ec_W$ (or α and θ_W). The electroweak symmetry breaking is parametrized by two more, $\mu^2 = -\lambda v^2$ and λ (or M_W and M_H). And the gauge-invariant Yukawa interactions of the Higgs doublet with fermions introduce most of the free parameters of the SM: 3 charged-lepton masses, 6 quark masses and 4 quark mixings. Therefore the electroweak lagrangian (132) depends on 17 parameters.^{vii} A practical set is:

$$\alpha = \frac{e^2}{4\pi}, \quad M_W = \frac{1}{2} g v, \quad M_Z = \frac{M_W}{c_W},$$

$$M_H = \sqrt{2\lambda} v, \quad m_f = \lambda_f \frac{v}{\sqrt{2}}, \quad \mathbf{U}_{\text{CKM}}. \quad (135)$$

Fortunately this not so small number of free parameters can be determined from very many different experiments, so the model is overconstrained and its predictions and self-consistency can be checked. It is only after the Higgs boson was discovered that all parameters have been measured. We present below what are the current experimental values of the most ‘influential’ parameters, and in the next section we elaborate on how this information is extracted from processes at increasing energy scales.

- *Fine structure constant.* The asymptotic value of the running α at zero momentum transfer can be estimated by several independent methods. One of the most precise determinations is based on the very accurate measurement of the electron anomalous magnetic moment (g_e) in a quantum cyclotron at Harvard, that is compared with a very accurate QED theoretical calculation [39],

$$[g_e] \quad \alpha^{-1} = 137.035\,999\,150 \quad (33). \quad (136)$$

This is compatible with the value of α that can be measured directly using the quantum Hall effect with larger uncertainty. Even more precise are other recent measurements based on photon recoil in atom interferometry with Cesium [40] and Rubidium [41], that are at present in conflict with one another,

$$[\text{Cs}] \quad \alpha^{-1} = 137.035\,999\,046 \quad (27),$$

$$[\text{Rb}] \quad \alpha^{-1} = 137.035\,999\,206 \quad (11). \quad (137)$$

- *Weak boson masses.* The SM predicts $M_W < M_Z$ (104) in agreement with measurements. The weak

gauge bosons were discovered at the Sp̄p̄S collider (CERN) in 1983 [42–45]. Today the weak boson masses are known with a precision of 0.1 per mille or better from combined measurements at the e^+e^- colliders LEP (CERN) and SLC (SLAC), and at the hadron colliders Tevatron (Fermilab) and LHC (CERN). The current world averages [26] are

$$M_W = 80.379 \pm 0.012 \text{ GeV [LEP2/Tevatron/LHC]},$$

$$M_Z = 91.1876 \pm 0.0021 \text{ GeV [LEP1/SLC]}. \quad (138)$$

- *Top quark mass.* The top is the only quark that is not confined in hadrons because being so heavy it weakly decays into a W boson and a b quark before hadronizing. It was discovered at the Tevatron in 1995 [46, 47]. Direct measurements of the kinematics of $t\bar{t}$ events are sensitive to what is usually interpreted as the pole mass. The current average [26] is:

$$m_t = 172.76 \pm 0.30 \text{ GeV [Tevatron/LHC]}. \quad (139)$$

- *Higgs boson mass.* The Higgs boson was discovered at the LHC in 2012 [48, 49] and its mass is already known at the permille level [26],

$$M_H = 125.25 \pm 0.17 \text{ GeV [LHC]}. \quad (140)$$

2.3.3. Observables and experiments

Low energy observables

At low momentum transfer $Q^2 \ll M_Z^2$ one can already get relevant information about the electroweak interactions. For example, the weak neutral currents were discovered by the observation of the elastic neutrino-electron scattering in the CERN bubble chamber detector Gargamelle in 1973 [50] (Fig. 12). The source of muon neutrinos, of energies less than 10 GeV, was a proton beam of 26 GeV from the PS accelerator. This was the confirmation of a cornerstone of the SM that won Glashow, Salam and Weinberg their Nobel prize, even before the W and the Z were found in $p\bar{p}$ collisions at a center-of-mass energy of 540 GeV ten years later. At present, very accurate measurements of the weak mixing angle θ_W come from the ratio of cross-sections $\sigma_{\bar{\nu}_\mu e}/\sigma_{\nu_\mu e}$ of neutrinos

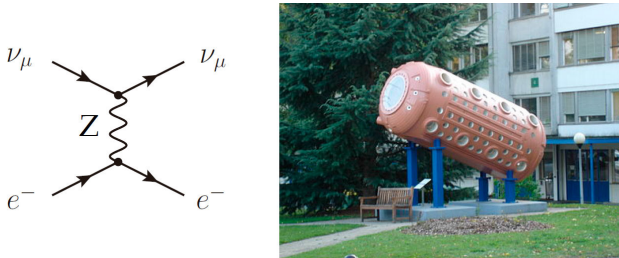


FIGURE 12. Weak neutral currents (left) discovered in the CERN bubble chamber detector Gargamelle (right).

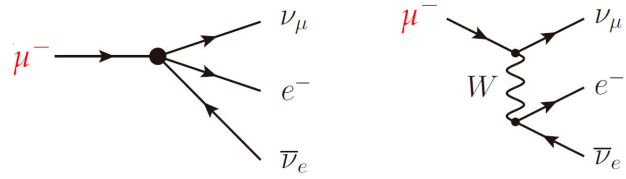


FIGURE 13. Muon decay in the 4-Fermi model (left) and tree-level contribution in the SM (right).

and antineutrinos in neutrino-electron scattering, and from the ratios of neutral to charged current cross-sections $\sigma_{\nu N}^{\text{NC}}/\sigma_{\nu N}^{\text{CC}}$ in neutrino-nucleon scattering at CERN and Fermilab.

The weak mixing angle can also be obtained from the left-right asymmetry (parity violation) in the cross-sections of polarized electrons off nucleons, $e_{R,L}N \rightarrow eX$, and from tiny parity violating effects induced by the weak interactions between electrons and quarks in heavy atoms (atomic parity violation), due to Z boson exchange, that grow with roughly the third power of the atomic number.

Valuable information comes from the measurement of the muon lifetime. The muon decay [51], together with the beta decay in Cobalt [52], provided the first confirmation of the violation of parity shortly after the seminal work of Yang and Lee [53] in 1956. The process $\mu \rightarrow e\bar{\nu}_e\nu_\mu$ proceeds at tree level in the SM through the exchange of a W boson with very low momentum transfer ($-q^2 \equiv Q^2 \leq m_\mu^2 \ll M_W^2$), and can be described by the effective 4-Fermi theory (proposed to explain the β decay in 1934 [54]) (Fig. 13),

$$i\mathcal{M} = -i\frac{4G_F}{\sqrt{2}} (\bar{e}\gamma^\rho\nu_L)(\bar{\nu}_L\gamma_\rho\mu)$$

$$= \left(\frac{ie}{\sqrt{2}s_W}\right)^2 \bar{e}_L\gamma^\rho\nu_L \frac{-ig_{\rho\delta}}{q^2 - M_W^2} \bar{\nu}_L\gamma^\delta\mu_L, \quad (141)$$

from which the Fermi constant G_F can be derived in terms of parameters of the fundamental theory,

$$\frac{G_F}{\sqrt{2}} = \frac{\pi\alpha}{2s_W^2M_W^2}. \quad (142)$$

The muon lifetime $\tau = \Gamma^{-1}$ is the inverse of its total decay width,^{viii}

$$\Gamma = \frac{G_F^2 m_\mu^5}{192\pi^3} f(m_e^2/m_\mu^2),$$

$$f(x) = 1 - 8x + 8x^3 - x^4 - 12x^2 \ln x, \quad (143)$$

where $f(m_e^2/m_\mu^2) = 0.99981295$ is a kinematic factor from phase space integration. The Fermi constant is measured very precisely from the muon lifetime at PSI in Villigen [26],

$$G_F = 1.166\,378\,7(6) \times 10^{-5} \text{ GeV}^{-2}. \quad (144)$$

It provides the value of the Higgs VEV (electroweak scale),

$$v = \left(\sqrt{2}G_F\right)^{-1/2} \approx 246 \text{ GeV} \quad (145)$$

and constrains the product $M_W^2 s_W^2$, which implies

$$M_Z^2 > M_W^2 = \frac{\pi\alpha}{\sqrt{2}G_F s_W^2} > \frac{\pi\alpha}{\sqrt{2}G_F} \approx (37.4 \text{ GeV})^2, \quad (146)$$

providing a lower limit of the weak boson masses, before their discovery. On the other hand, since we have now independent measurements of G_F , α , M_W and M_Z one can attempt a first consistency check of the model by comparing the value of G_F in (144) with the prediction using the *tree-level* expression (142) and $s_W^2 = 1 - M_W^2/M_Z^2$,

$$G_F = \frac{\pi\alpha}{\sqrt{2}(1 - M_W^2/M_Z^2)M_Z^2} \approx 1.125 \times 10^{-5}. \quad (147)$$

The glaring discrepancy will disappear when quantum corrections are included (see Sec. 2.3.4).

Fermion-pair production in e^+e^- colliders

Lepton colliders provide a clean environment to study the electroweak interactions. In particular, the e^+e^- annihilation into a fermion-antifermion pair is given, at tree level, by the exchange of a photon and a Z boson in the s -channel. At increasing center-of-mass energies the cross-section falls like $1/s$ dominated by the virtual photon exchange while the Z exchange becomes more important until it reaches a maximum right at $s = M_Z^2$ where it presents a resonance peak (Fig. 14).

It is a good exercise to try and reproduce the differential cross-section for $e^+e^- \rightarrow \bar{f}f$ (in the case of unpolarized fermions),

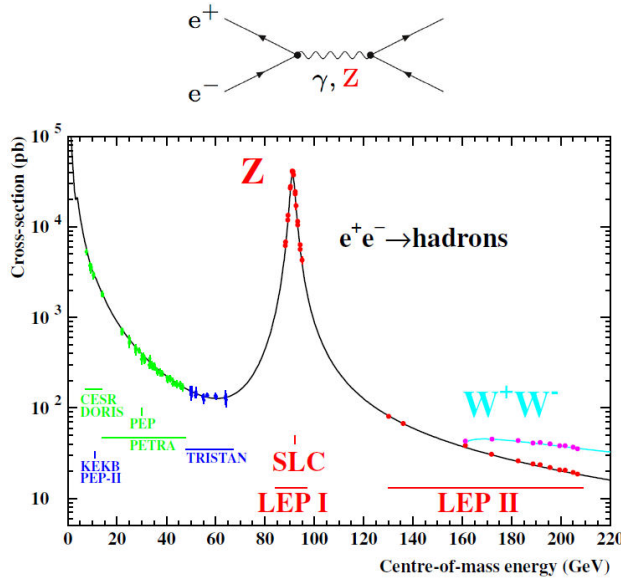


FIGURE 14. Top: Tree-level contributions to fermion-pair production in e^+e^- collisions. Bottom: Hadronic cross-section as a function of the center-of-mass energy. The solid line is the SM prediction, and the points are the experimental measurements at different colliders, whose energy ranges are also indicated. From Ref. [55].

$$\frac{d\sigma}{d\Omega} = N_c^f \frac{\alpha^2}{4s} \beta_f \left\{ [1 + \cos^2 \theta + (1 - \beta_f^2) \sin^2 \theta] G_1(s) + 2(\beta_f^2 - 1)G_2(s) + 2\beta_f \cos \theta G_3(s) \right\},$$

$$G_1(s) = Q_e^2 Q_f^2 + 2Q_e Q_f v_e v_f \text{Re}\chi_Z(s) + (v_e^2 + a_e^2)(v_f^2 + a_f^2)|\chi_Z(s)|^2,$$

$$G_2(s) = (v_e^2 + a_e^2)a_f^2|\chi_Z(s)|^2,$$

$$G_3(s) = 2Q_e Q_f a_e a_f \text{Re}\chi_Z(s) + 4v_e v_f a_e a_f |\chi_Z(s)|^2, \quad (148)$$

where $\chi_Z(s) \equiv s/(s - M_Z^2 + iM_Z\Gamma_Z)$ contains the Z propagator including an imaginary part relevant in the vicinity of the resonance, $N_c^f = 1$ (3) for $f = \text{lepton}$ (quark), v_f and a_f are the vector and axial-vector couplings (96) and $\beta_f = \sqrt{1 - 4m_f^2/s}$ is the final fermion velocity in the center of mass frame (the electron mass can be safely neglected). The contribution of each diagram and their interference is evident and the parity violation due to the Z exchange manifests itself as a forward-backward asymmetry: the term proportional to $\cos \theta$ involving both vector and axial vector couplings. Integrating over the solid angle, the total cross-section

$$\sigma(s) = N_c^f \frac{2\pi\alpha^2}{3s} \beta_f \times [(3 - \beta_f^2)G_1(s) - 3(1 - \beta_f^2)G_2(s)], \quad (149)$$

gives the profile of Fig. (14). The (inclusive) hadronic cross-section is obtained by summing over all quark flavors above threshold at a given energy, essentially five in the displayed range.

Z pole observables

On the resonance peak ($s = M_Z^2$) the Z propagator becomes purely imaginary, the interference of the photon and Z exchange diagrams vanishes and the cross-section is dominated by the weak interaction (the QED contribution is suppressed by a factor $(\Gamma_Z/M_Z)^2 \lesssim 10^{-3}$). This was the energy domain of the first phase (1989-1995) of the circular e^+e^- collider LEP at CERN and the linear collider SLC (1992-1998) at SLAC. The former collected 17 million Z decays at center-of-mass energies within plus or minus 3 GeV of the Z pole, and the latter only 600 thousand but with a longitudinally polarized electron beam. At these colliders very precise measurements of various Z pole observables have been performed. These include the Z mass M_Z , the total width Γ_Z , and partial widths $\Gamma_{\bar{f}f}$ for $Z \rightarrow \bar{f}f$. It is customary to introduce

$$\sigma_{\text{had}}^0 \equiv 12\pi \frac{\Gamma_{e^+e^-} \Gamma_{\text{had}}}{M_Z^2 \Gamma_Z^2},$$

$$R_\ell \equiv \frac{\Gamma_{\text{had}}}{\Gamma_{\ell^+\ell^-}}, \quad R_q \equiv \frac{\Gamma_{q\bar{q}}}{\Gamma_{\text{had}}}, \quad (150)$$

where $\ell = e, \mu, \tau, q = b$ or c and Γ_{had} is the partial width into hadrons.^{*iX*} The effects of the photon-exchange diagram are subtracted in σ_{had}^0 . Very useful constraints follow from various Z pole (forward-backward and left-right) asymmetries,

$$A_{\text{FB}}^f = \frac{\sigma(\cos\theta > 0) - \sigma(\cos\theta < 0)}{\sigma(\cos\theta > 0) + \sigma(\cos\theta < 0)} = \frac{3}{4} A_f \frac{A_e + P_e}{1 + P_e A_e},$$

$$A_{LR} = \frac{\sigma_L - \sigma_R}{\sigma_L + \sigma_R} = A_e P_e, \quad (151)$$

where P_e is the initial electron polarization and

$$A_f \equiv \frac{2v_f a_f}{v_f^2 + a_f^2}. \quad (152)$$

By measuring the Z pole observables (150) one can estimate the Z invisible width, $\Gamma_{\text{inv}} = \Gamma_Z - \Gamma_{e^+e^-} - \Gamma_{\mu^+\mu^-} - \Gamma_{\tau^+\tau^-} - \Gamma_{\text{had}}$, that can be used to deduce the number of light neutrino species, $N_\nu = \Gamma_{\text{inv}}/\Gamma_{\nu\bar{\nu}}$, from the partial width to neutrinos predicted by the SM. The overall scale of the Z lineshape is fixed by the peak cross-section σ_{had} , whose experimental value is extracted from the number of observed hadronic events given the collider luminosity, that in turn is measured from the rate of $e^+e^- \rightarrow e^+e^-$ events at low angle provided the (accurate enough) theoretical prediction of the Bhabha scattering cross-section. The combination of the measurements made by the four LEP experiments (Fig. 15) led to $N_\nu = 2.9840 \pm 0.0082$ [55], two standard deviations away from 3.0, the number of fermion generations in the SM. Very recently the prediction for the Bhabha cross-section was found to be overestimated, and consequently the luminosity

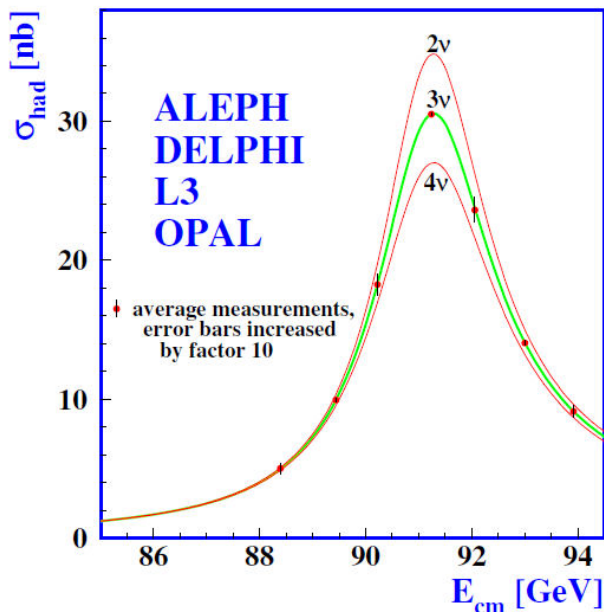


FIGURE 15. Measurements of the hadron production cross-section around the Z resonance (lineshape) at LEP. The curves indicate the predicted cross-section for two, three and four neutrino species with SM couplings and negligible mass. From Ref. [55].

underestimated [56]. The new analysis of the Z lineshape fit, reducing σ_{had} while slightly increasing Γ_Z , yields the result $N_\nu = 2.9963 \pm 0.0074$, hence putting an end to the 2σ tension with the SM.

W boson production

LEP2 (1996-2000) operated at higher center-of-mass energies (Fig. 14) to study W -pair production (Fig. 16), and in part also to search (unsuccessfully) for the Higgs boson [57]. Particularly important was the exploration of the W^+W^- threshold (161 GeV), where the dependence of the cross-section with the W mass is large, that allowed to determine M_W very precisely. At higher energies (172 to 209 GeV) this dependence is much weaker and W bosons were directly reconstructed and their mass determined from the invariant mass of the decay products. LEP2 was also the first to probe the triple gauge couplings $WW\gamma$ and WWZ , predicted by the non-abelian gauge symmetry (Fig. 16), another milestone of the SM.

In hadron colliders, on-shell W bosons are tagged by their decay into charged leptons with high transverse momentum (Fig. 17). The values of the W mass from Tevatron and LHC are compatible with the measurements from LEP2 and have at present very similar precision.

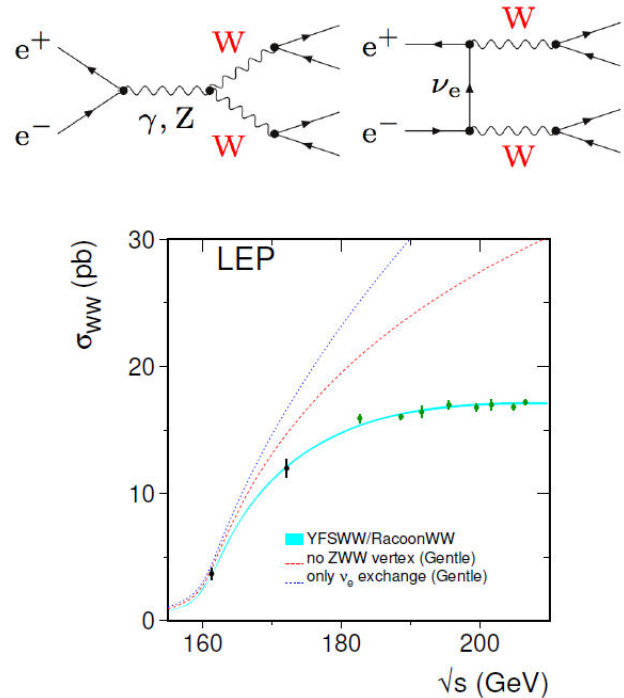


FIGURE 16. Top: Tree-level contributions to $e^+e^- \rightarrow W^+W^-$. Bottom: Measurements of the W -pair production cross-section at LEP2, compared to theoretical predictions (taking $M_W = 80.35$ GeV) including all diagrams (cyan), removing the ZWW vertex (red), and assuming only the $\bar{\nu}_e$ exchange (blue). From Ref. [57].

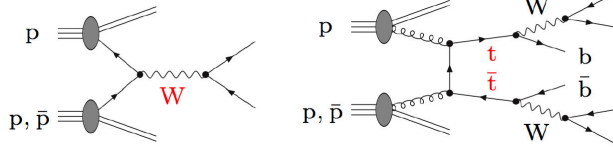


FIGURE 17. W production and top-quark production at hadron colliders.

Top quark production

Top quarks are produced in hadron colliders dominantly in pairs through the strong processes $q\bar{q} \rightarrow t\bar{t}$ (Fig. 17) and $gg \rightarrow t\bar{t}$ at leading order. At Tevatron ($p\bar{p}$, $\sqrt{s} = 1.96$ TeV) 85% of the production cross-section is from $q\bar{q}$ annihilation, while at LHC (pp) about 90% ($\sqrt{s} = 7$ TeV) or 80% ($\sqrt{s} = 14$ TeV) comes from from gluon fusion. Single-top quarks are also produced in electroweak processes, $q\bar{q}' \rightarrow t\bar{b}$, $qb \rightarrow q't$, $bg \rightarrow Wt$, with somewhat smaller cross-sections. The top-quark mass is kinematically reconstructed from invariant mass distributions of the final states in different decay channels.

Higgs boson production

The Higgs boson is the smoking gun providing evidence that the spontaneous breaking of the electroweak symmetry *does* generate the masses of weak bosons and fermions. The Higgs mechanism is essential not only because the renormalizability of the SM is then guaranteed [16], a requirement that is nowadays not considered so crucial as in former times [58], but also because it ensures the unitarity of the model [59]: the scattering amplitudes have a good behavior at high energy because of ‘miraculous’ cancellations that follow when the electroweak boson self-interactions are of the Yang-Mills form,^x as prescribed by the gauge symmetry

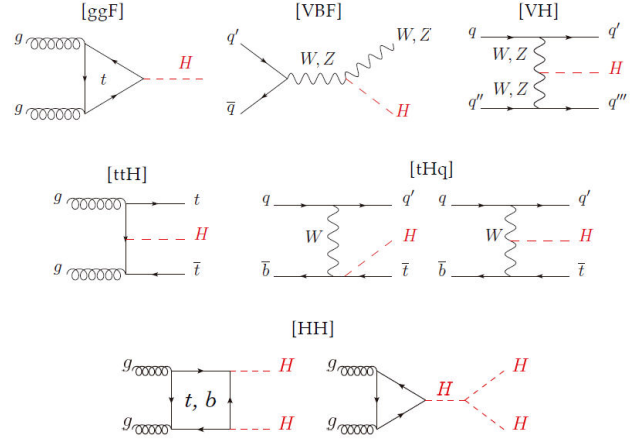


FIGURE 18. Leading-order diagrams for Higgs production mechanisms at hadron colliders: gluon fusion [ggF], vector boson fusion [VBF], Higgs-strahlung [VH], associated production with a pair of top quarks [ttH] or a single top quark [tH] and Higgs boson pair production [HH]. From Ref. [26].

(e.g. $e^+e^- \rightarrow W^+W^-$) and scalar-exchange diagrams of the Higgs type are included (e.g. $W^+W^- \rightarrow W^+W^-$). After its long awaited discovery, the predicted properties of the SM Higgs boson [60] can finally be checked against experiment.

The main production mechanisms at the Tevatron^{xi} and the LHC are gluon fusion, weak-boson fusion, associated production with a gauge boson, and associated production with a pair of top quarks or with a single top quark (see Fig. 18). The Higgs boson pair production in the SM is more rare but very important because it allows to check the trilinear Higgs boson self-coupling. The production cross-sections in pp collisions at LHC energies and the branching ratios for the decay of a Higgs boson with a mass around 125 GeV are shown in Fig. 19. The Higgs boson is mostly produced by gluon fusion (gluons are the most abundant parton in the proton at low $x \sim M_H/\sqrt{s}$) mediated by a top-quark loop

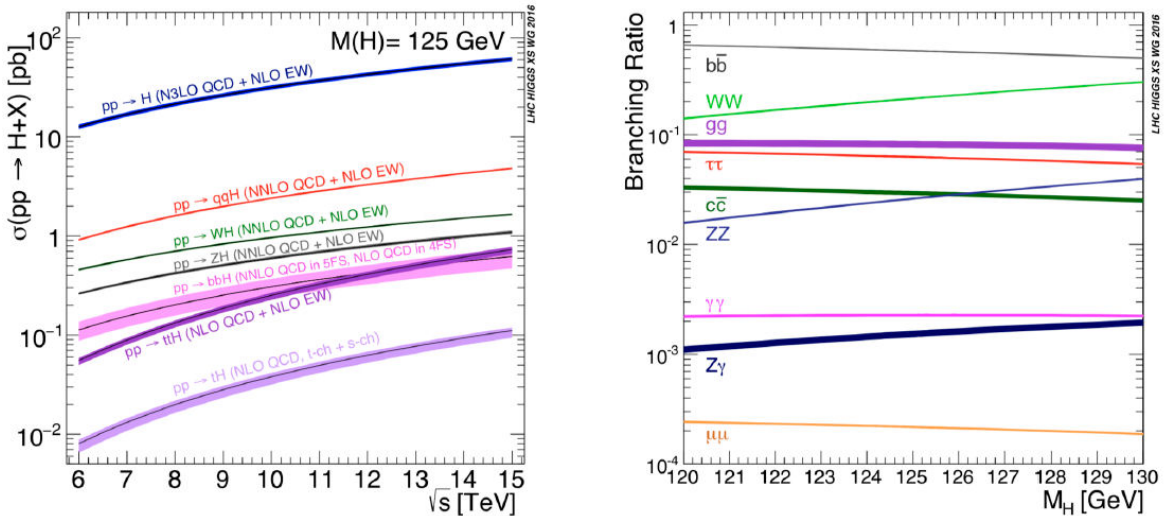


FIGURE 19. Higgs boson production cross-sections as a function of the LHC center of mass energy (left) and Higgs boson branching ratios for the mass range around 125 GeV (right). From Ref. [61].

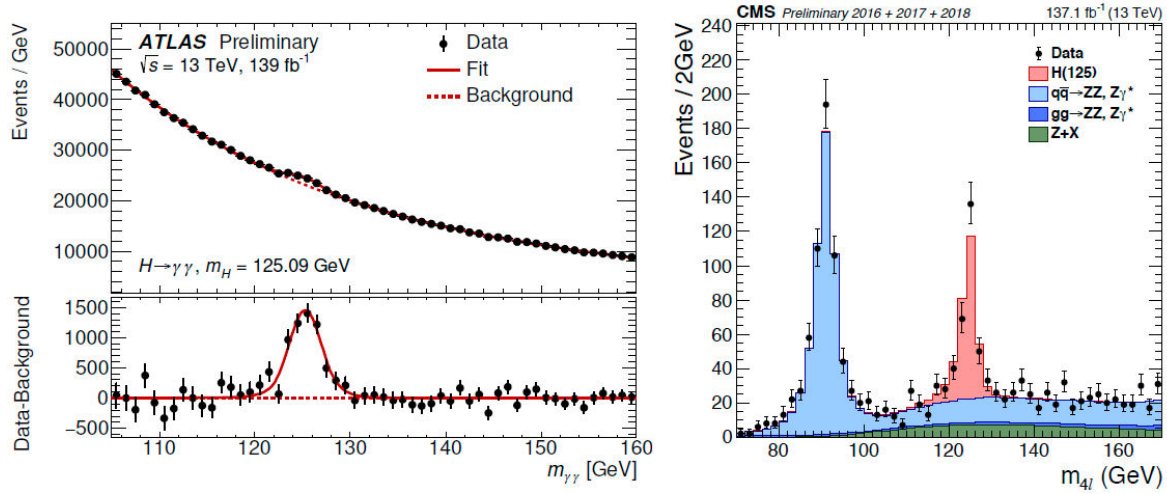


FIGURE 20. Left: Invariant diphoton mass distribution observed by ATLAS [64]. Right: invariant m_{4l} distribution from CMS [65]. They exhibit clear signals of $H \rightarrow \gamma\gamma$ and $H \rightarrow ZZ^* \rightarrow 4l$, respectively, allowing to measure the Higgs boson mass.

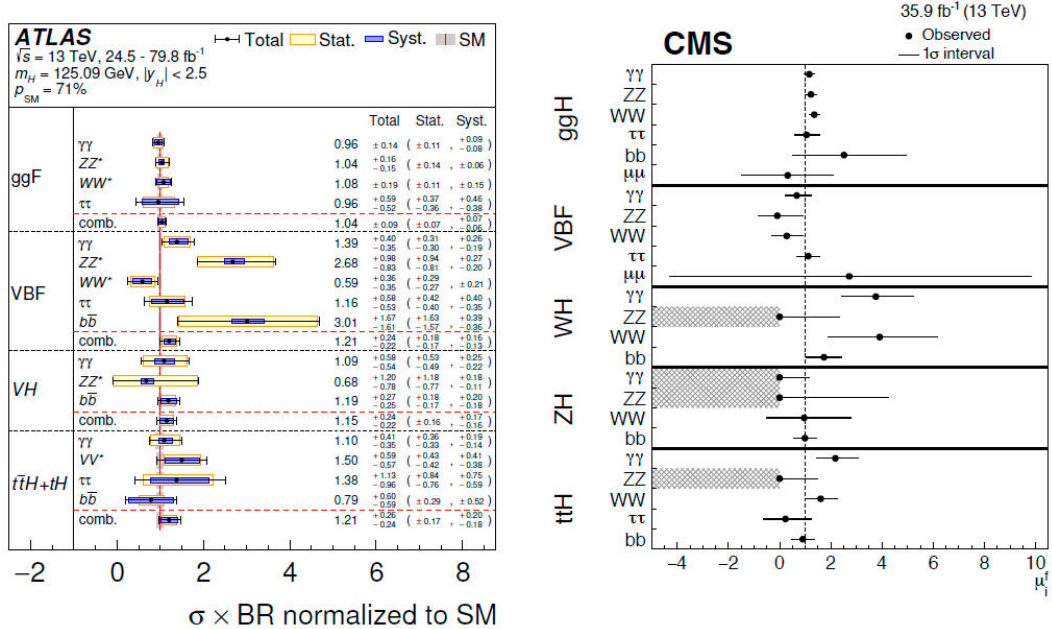


FIGURE 21. Combined measurements of the signal strengths for the five main production and five main decay modes. The hatched combinations require more data. From Ref. [26].

(whose heavy mass enhances the effective coupling). The dominant decay channel is $H \rightarrow b\bar{b}$ (about 58%) but it suffers from large backgrounds. Less probable are $H \rightarrow ZZ^*$, WW^* (with one of the gauge bosons off-shell) and $H \rightarrow \gamma\gamma$ but they provide cleaner signals and played an important role in the Higgs discovery. In fact, the decay into $b\bar{b}$ has been discovered (significance above 5σ) as recently as 2018 [62]. At the other end, there is ‘evidence’ for the $\mu\mu$ channel (significance above 3σ) from 2020 [63].

The current average value of the Higgs boson mass comes from the combination of mass measurements in the $\gamma\gamma$ and ZZ channels (Fig. 20).

The Higgs event rates are proportional to the production cross-sections times the branching ratios (BR). Experimental results are often normalized to the SM predictions and expressed in terms of signal strengths $\mu = (\sigma \times \text{BR})_{\text{obs}} / (\sigma \times \text{BR})_{\text{SM}}$. Figure 21 shows that data are in fair agreement with predictions for a good number of channels and production mechanisms.

As for the tests of Higgs couplings, recall that in the SM the Yukawa coupling between the Higgs boson and the fermions is proportional to the fermion mass (m_F), while the coupling to weak bosons is proportional to the square of the vector boson masses (m_V). Then one may define $y_F \equiv \kappa_F m_F / v$ for fermions and $y_V \equiv \sqrt{\kappa_V} m_V / v$ for weak

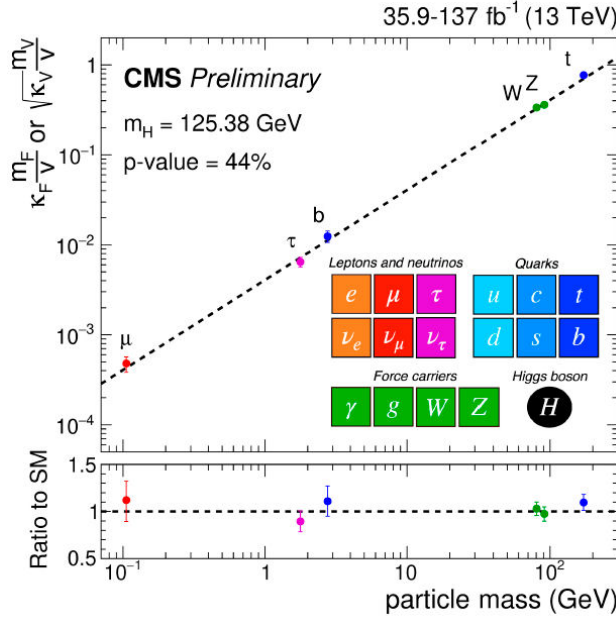


FIGURE 22. Best fit estimates for the Higgs coupling strengths to fermions and gauge bosons. From Ref. [63].

bosons where κ_F and κ_V are coupling strengths that measure the ratio of observations to SM predictions. The Higgs couplings to fermions and gauge bosons have been probed over more than three orders of magnitude with no significant deviations from the SM (Fig. 22).

2.3.4. Precise determination of parameters

Experimental precision requires accurate theoretical predictions, that are based on calculations beyond the tree-level approximation. The trouble is that the computation of loop corrections is laborious and plagued of infinities which involves the extra complication of renormalization.

A good example of the need for quantum corrections is the derivation of the Fermi constant from the measurement of the muon lifetime that follows from the identification

$$G_F = \frac{\pi\alpha}{\sqrt{2}(1 - M_W^2/M_Z^2)M_W^2} (1 + \Delta r[m_t, M_H]), \quad (153)$$

where Δr depends on the masses and couplings of virtual particles exchanged in the loop as in Fig. 23. This correction will fill the gap between (144) and (147).

Actually, since the muon lifetime is measured more precisely than M_W , the W mass can be independently obtained from the expression of G_F in Eq. (153) that implies

$$M_W^2(\alpha, G_F, M_Z, m_t, M_H) = \frac{M_Z^2}{2} \left(1 + \sqrt{1 - \frac{4\pi\alpha}{\sqrt{2}G_F M_Z^2} [1 + \Delta r(m_t, M_H)]} \right), \quad (154)$$

introducing a correlation between M_W , m_t and M_H , given α , G_F and M_Z . This correlation has historically served as a

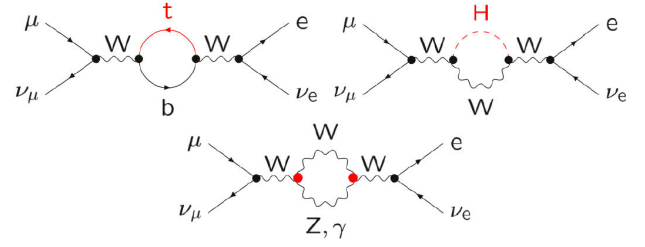


FIGURE 23. One-loop corrections to the muon decay amplitude.

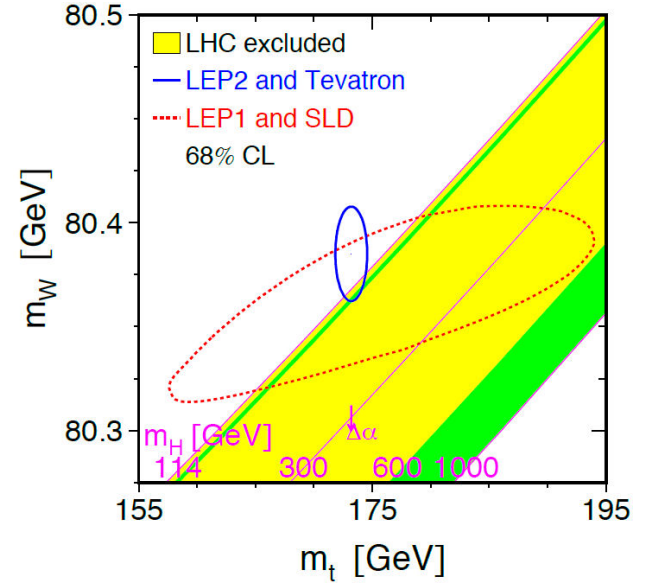


FIGURE 24. Indirect constraints on M_W and m_t from LEP1/SLC data (dashed contour) and direct measurements from LEP2/Tevatron data (solid contour). Also shown is the relation between both masses and the Higgs mass (solid lines), the region allowed by direct Higgs searches (dark green bands) and the region excluded by the LHC right before the Higgs boson discovery. From Ref. [57].

handle to constrain yet unknown parameters from the value of others. As an example, in Fig. 24 by the LEP Electroweak Working Group [57] shows the comparison of indirect and direct constraints on M_W and m_t from LEP and Tevatron together with the region of Higgs masses consistent with precision tests before the Higgs boson was found at the LHC.

Another example is the corrections to vector and axial-vector couplings from Z pole observables,

$$v_f \rightarrow g_V^f = v_f + \Delta g_V^f \quad a_f \rightarrow g_A^f = a_f + \Delta g_A^f, \quad (155)$$

that lead to a fermion-dependent effective weak mixing angle given by

$$\begin{aligned} \sin^2 \theta_{\text{eff}}^f &\equiv \frac{1}{4|Q_f|} \left| 1 - \text{Re}(g_V^f/g_A^f) \right| \\ &\equiv s_W^2 (1 + \Delta\kappa_Z^f), \end{aligned} \quad (156)$$

where $\Delta\kappa_Z^f$ is the quantum correction in the $\overline{\text{MS}}$ renormalization scheme and $s_W^2 = 1 - (M_W^2/M_Z^2)$ is the tree-level

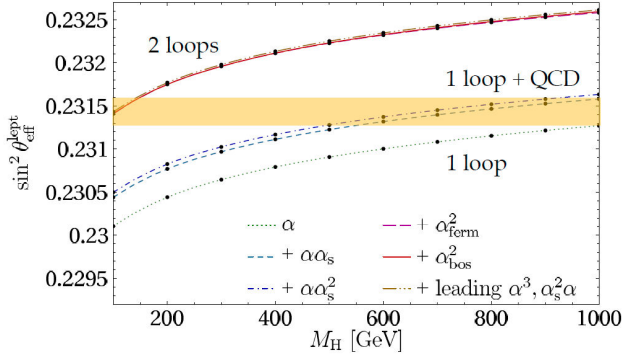


FIGURE 25. Contribution of several orders of radiative corrections to the effective leptonic weak mixing angle $\sin^2 \theta_{\text{eff}}^{\text{lept}}$ as a function of the Higgs mass. The tree-level value $s_W^2 = 1 - M_W^2/M_Z^2 \approx 0.2290$ is below the range shown. The yellow band is the experimental accuracy at the time, $\sin^2 \theta_{\text{eff}}^{\text{lept}} = 0.23147 \pm 0.000017$. From Ref. [66].

value. As shown in Fig. 25, the effective leptonic weak mixing angle has been measured with high precision and at least two-loop calculations are needed [66] to get a prediction compatible with experiment, already pointing to a light Higgs mass (the remaining theoretical uncertainty from unknown higher-order corrections was estimated to be 4.7×10^{-5}).

There are also experiments and observables testing the flavor structure of the SM, either flavor-conserving, like dipole moments, or flavor-changing, like $B_s \rightarrow X_s \gamma$ and many other hadron and lepton decays. They are very sensitive to new physics through loop corrections. As already mentioned, the extremely precise measurement of the electron anomalous magnetic moment $a_e = (g_e - 2)/2$,

$$a_e^{\text{exp}} = 0.001\,159\,652\,182\,032 \quad (720), \quad (157)$$

is used to estimate the fine structure constant α from the QED prediction at 5 loops [39]. On the other hand, the anomalous magnetic moment of the muon was measured at Brookhaven with very high precision [67]

$$a_\mu^{\text{exp}} = 116\,592\,089 \quad (63) \times 10^{-11} \quad [\text{BNL}], \quad (158)$$

but it does not match the SM prediction, a puzzle that has survived for almost two decades. The most recent calculation by the Muon $g - 2$ Theory Initiative [68] yields

$$a_\mu^{\text{SM}} = 116\,591\,810 \quad (43) \times 10^{-11}, \quad (159)$$

that gives $a_\mu^{\text{exp}} - a_\mu^{\text{SM}} = 279 \quad (76) \times 10^{-11}$, a 3.7σ deviation. Very recently a new experiment at Fermilab has released its first results [69],

$$a_\mu^{\text{exp}} = 116\,592\,061 \quad (41) \times 10^{-11} \quad [\text{FNAL}], \quad (160)$$

compatible with the previous measurements and increasing the discrepancy to 4.2σ (Fig. 26). This is nowadays considered a compelling evidence of physics beyond the SM.

Another playground where precision physics has revealed departures from the SM predictions is b -hadron decays, with

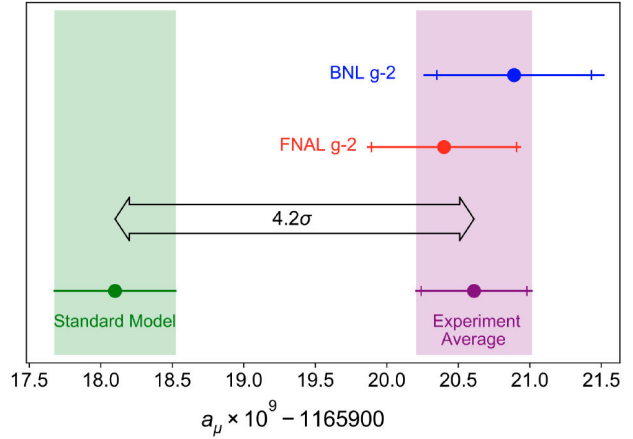


FIGURE 26. Experimental values of a_μ from Brookhaven, Fermilab and combined average. The inner tick marks indicate the statistical contribution to the total uncertainties. The recommended value for the standard model prediction [68] is also shown.

tensions in rare flavor-changing neutral currents and in tree-level semileptonic decays that constitute the so-called flavor anomalies in B-physics (see [71] for a recent review). They have been observed in measurements of branching fractions and angular observables, as well as in lepton flavor universality tests. A good example of the latter is the measurement by LHCb [70] of the ratio

$$R_K = \frac{\text{BR}(B^+ \rightarrow K^+ \mu^+ \mu^-)}{\text{BR}(B^+ \rightarrow K^+ e^+ e^-)} = 0.846_{-0.041}^{+0.044}, \quad (161)$$

that is about 3σ from the SM prediction, 1.00 ± 0.01 , providing evidence for the violation of lepton universality in these decays. This tension, that was not significant in previous measurements at BaBar (SLAC) and Belle (KEK), has survived and even grown with increasing statistics at LHCb (Fig. 27). More data from LHCb and the forthcoming Belle II experiment [72] will establish whether this anomaly must be taken seriously.

2.3.5. Global fits

As we have seen, precision measurements test the SM at the quantum level, which allows to perform consistency checks among the results. The global fits consist of finding the values of a set of input parameters that minimize the χ^2 accounting for the deviation between a number of precision observables and their SM predictions. The predictions are given by theoretical expressions that are functions of the input parameters. The precision observables are sometimes more appropriately named ‘pseudo-observables’ because they are not directly experimental observables but derived quantities depending on the order of perturbation theory and on the choice of renormalization scheme.

The latest electroweak global fit by Gfitter [73], using the observables $M_H, M_W, \Gamma_W, M_Z, \Gamma_Z, \sigma_{\text{had}}, R_{\ell,c,b}, A_{\text{FB}}^{0,\ell}, A_{\text{FB}}^{0,c}, A_{\text{FB}}^{0,b}, A_\ell, A_c, A_b, \sin^2 \theta_{\text{eff}}^\ell, m_c, m_b, m_t, \alpha(M_Z^2)$ and

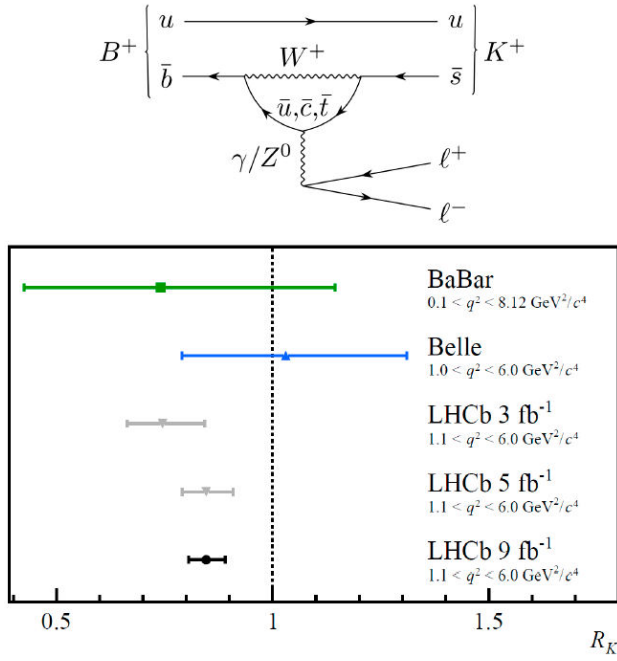


FIGURE 27. Fundamental processes contributing to $B^+ \rightarrow K^+ \ell^+ \ell^-$ decays in the SM and comparison between R_K measurements. From Ref. [70].

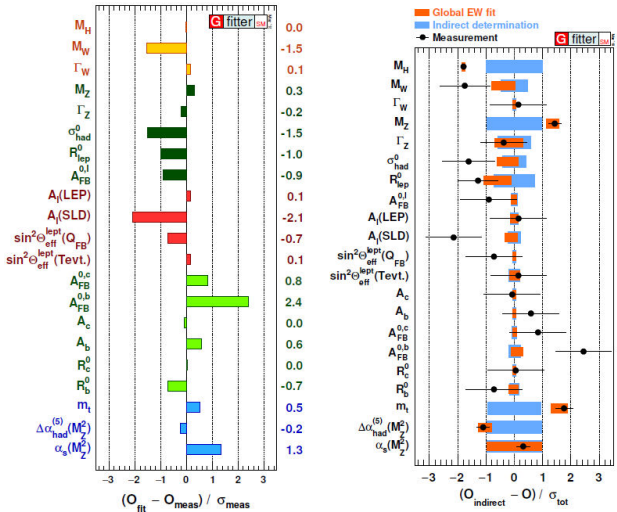


FIGURE 28. Left: Comparing fit results with direct measurements. Right: Comparing fit results (orange bars) with indirect determinations (blue bars) and direct measurements (data points). The total error is the error of the direct measurement added in quadrature with the error from the indirect determination. From Ref. [73].

$\alpha_s(M_Z^2)$, converges to a $\chi^2_{\min} = 18.6$ for 15 degrees of freedom (number of fit observables minus number of free parameters). This corresponds to a p -value of 0.23. The p -value tests the likelihood of the null-hypothesis, the probability of obtaining data equal or less compatible with the theory, so the lower the better.

It is also interesting to compare the fit results with the input measurements [73]. The left panel of Fig. 28 shows the deviations between global fit values and direct measurements

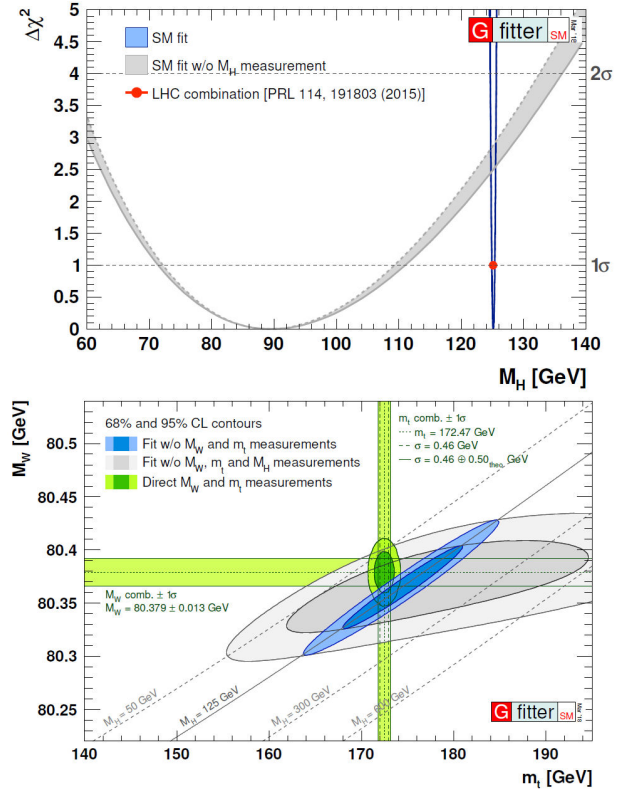


FIGURE 29. Top: $\Delta\chi^2$ as a function of Higgs boson mass for a global SM fit with and without the M_H measurement (blue and grey bands). Bottom: Contours of 68% and 95% confidence level obtained from scans of fits with fixed variable pairs M_W, m_t . The narrower blue and larger grey allowed regions are the results of the fit including and excluding the M_H measurement, respectively. From Ref. [73].

in units of the experimental uncertainty. There are some tensions but none above 3σ . The right panel of Fig. 28 shows the difference between the global fit results (orange bars) as well as the input measurements (data points) with the indirect determinations (blue bars). The indirect determinations are the best fit values without using the constraint from the corresponding input measurement. This illustrates the impact of indirect uncertainties on total uncertainties. Finally, the top panel of Fig. 29 shows that the global fit to the SM prefers a somewhat lighter Higgs boson. The bottom panel is an updated version of the confidence level profile of M_W versus m_t in Fig. 24 where the M_H measurement at LHC is included in the fit or not (blue or grey contour). The good agreement of both contours with the direct measurements (green bands and ellipse for two degrees of freedom) is the ultimate confirmation of the consistency of the SM.

3. Concluding remarks

The Standard Model of the electroweak and strong interactions of particle physics is a relativistic quantum field theory based on a gauge symmetry that is spontaneously broken by the Brout-Englert-Higgs mechanism. As a consequence it is

renormalizable and fully predictive. It has been confirmed by a plethora of low and high energy experiments with remarkable accuracy, at the level of quantum corrections, with (almost) no significant deviations.

However, in spite of its tremendous success, the SM leaves fundamental questions unanswered: why three generations? what is the reason for the observed pattern of quark and lepton masses and mixings? And more importantly, there are several hints for physics beyond. Some are phenomenological and others more conceptual. Perhaps the most compelling is the muon magnetic dipole moment, whose very precise measurement is still challenging the SM prediction after many years of efforts both from the experimental and the theory side. There is also a bunch of flavor anomalies in B physics that are gaining evidence. The neutrino sector is without doubt the Achilles heel of the model, that has already required an extension to accommodate neutrino masses and mixings in order to explain the flavor oscillations. The possibility that neutrinos are Majorana fermions, theoretically well motivated and under intense experimental exploration, would open the window to lepton number violation and, linked to this, would suggest the existence of extra neutrinos at a very heavy scale that might contribute to solve the baryon asymmetry problem^{xiii} [74] through leptogenesis [75]. Another problem is dark matter. If it is composed of hypothetical particles interacting with ordinary matter only through gravity [76], the SM does not provide any appropriate candidate, although there are interesting alternatives [77]. Nonetheless, it is very suggestive that the most popular solution to the strong CP problem (the Peccei-Quinn mechanism [78]) introduces a new global anomalous symmetry spontaneously broken at low energies giving rise to a pseudo-Goldstone boson, the axion, considered a viable candidate for dark matter.

Of course the SM cannot be the ‘theory of everything’, since it does not include the gravitational interaction that governs the universe dynamics at large scales. But it has something to say about the value of the vacuum energy density, ρ_{vac} , that is related to the cosmological constant by $\Omega_\Lambda = \rho_{\text{vac}}/\rho_c$ where $\rho_c = 3H_0^2/(8\pi G_N)$ is the critical density of the universe. The cosmological constant is the simplest form of dark energy [79] so far indistinguishable from the more general quintessence. According to current cosmological measurements of the cosmic expansion acceleration [80], $\Omega_\Lambda \approx 0.7$, that implies $\rho_{\text{vac}} \approx (2 \times 10^{-3} \text{ eV})^4$. In the SM, as in any quantum field theory, the values of quantities like the masses, couplings or the cosmological constant cannot be predicted. They are fixed by the renormalization procedure: the bare parameters are chosen so that they cancel the divergent corrections and leave us with the desired renormalized quantity. The computation of the vacuum energy density yields a result that diverges quartically with the cutoff (physics scale up to which the theory is meaningful),

$$\rho_{\text{vac}} \approx \rho_0(\Lambda_{\text{cut}}) + c\Lambda_{\text{cut}}^4. \quad (162)$$

If we assume no new physics until the Planck scale ($\Lambda_{\text{cut}} \sim M_P \sim 10^{19} \text{ GeV}$), where gravity becomes relevant, then

$\rho_0(\Lambda_{\text{cut}})$ has to be chosen so that a very fine-tuned cancellation with the correction of more than 120 digits will be required. Even if new physics were behind the corner, say $\Lambda_{\text{cut}} \sim 1 \text{ TeV}$, the fine-tuning would be of about 60 digits. Although $\rho_0(\Lambda_{\text{cut}})$ has no physical meaning and can be chosen at will, this level of fine-tuning is considered very unnatural.

Another naturalness problem of the SM has to do with the renormalization of the mass of scalar fields. The corrections to the mass squared of a scalar field, like the Higgs, diverge quadratically with the cutoff,

$$M_H^2 \approx (M_H^0)^2(\Lambda_{\text{cut}}) + c\Lambda_{\text{cut}}^2. \quad (163)$$

This is in contrast to the masses of fermion or gauge fields whose corrections grow only logarithmically with the cutoff, because they are protected by a symmetry (they would be massless if chiral or gauge symmetries were unbroken). If we take $\Lambda_{\text{cut}} \sim M_P$ then a cancellation of 34 digits is needed to match the observed Higgs mass $M_H \simeq 125 \text{ GeV}$. However, this hierarchy problem is different from the cosmological constant problem, because it could be solved if there were new physics not far above the electroweak scale (at $\Lambda_{\text{cut}} \sim 1 \text{ TeV}$ for example) as in the case of supersymmetric extensions of the SM [81], or if the ‘true’ Planck scale is $M_P \sim 1 \text{ TeV}$ as in the case of models with extra dimensions [82, 83]. Unfortunately there is no experimental clue of any of them.

In the absence of signals from a better fundamental theory that can tie up the loose ends of the SM, we can always consider the SM as a low-energy effective field theory [84, 85] (SMEFT) valid up to some energy scale, like the 4-Fermi model is a good effective theory for $E \ll M_W$. The effective lagrangian can be written as

$$\mathcal{L} = \mathcal{L}_{\text{SM}} + \sum_{i,n} \frac{c_i^{(n)} \mathcal{O}_i^{(n)}}{\Lambda_{\text{NP}}^{n-4}}, \quad (164)$$

where \mathcal{L}_{SM} is the renormalizable part of the lagrangian, that we had so far identified with the SM. The new physics is parametrized by a set of higher dimensional (Lorentz and gauge invariant) operators $\mathcal{O}_i^{(n)}$ made of SM fields, where $n > 4$ is the canonical dimension. Λ_{NP} is the new physics scale, such as the mass of a new particle. Their effects are suppressed by $(E/\Lambda_{\text{NP}})^{n-4}$ with respect to the SM operators where E is any low energy scale or mass, so the higher the dimension of the operator the smaller its contribution at low energies. Therefore, given a finite experimental precision we only need operators up to certain dimension and, since there are a finite number of these, their coefficients can be renormalized. The lack of predictivity on the (remaining) coefficients above some order is irrelevant. This is why the SMEFT, though ‘non-renormalizable’, is perfectly acceptable to describe physics below Λ_{NP} and is used as a very powerful framework [86].

Acknowledgments

I would like to thank the students who attended these lectures for their questions and comments, and the organizers of the School for their kind invitation. I am indebted to Alejandro Jiménez Cano for many fruitful discussions and

his help to prepare this manuscript. This work was supported in part by the Spanish Ministry of Science, Innovation and Universities (FPA2016-78220-C3, PID2019-107844GB-C21/AEI/10.13039/501100011033), and by Junta de Andalucía (FQM 101, SOMM17/6104/UGR, P18-FR-1962, P18-FR-5057).

-
- i.* Natural units $\hbar = c = 1$ are used throughout this course.
 - ii.* If we take any complex value $|v|e^{i\alpha}$ the conclusions will be the same for redefined fields, $\eta \rightarrow (\eta \cos \alpha - \chi \sin \alpha)$ and $\chi \rightarrow (\eta \sin \alpha + \chi \cos \alpha)$.
 - iii.* The signs of g and g' are conventional, with no effect on physical observables.
 - iv.* The so-called Weinberg angle was actually introduced by S. L. Glashow [17].
 - v.* For instance, if the symmetry breaking is triggered by a complex Higgs triplet one gets $\rho = 1/2$.
 - vi.* An additional constant term $(1/4)\lambda v^4 \equiv -\rho_0$ has been omitted. It is irrelevant for the field dynamics but provides a (negative) contribution to the vacuum energy density. See discussion in Sec. 3.
 - vii.* If light neutrino masses and mixings are included, add 3 more masses and 4 (or 6 for the Majorana case) parameters in the PMNS matrix.
 - viii.* The process $\mu \rightarrow e\bar{\nu}_e\nu_\mu$ is by far the dominant decay channel. The decays $\mu \rightarrow e\bar{\nu}_e\nu_\mu e^+e^-$ and $\mu \rightarrow e\bar{\nu}_e\nu_\mu\gamma$ with branching ratios $\sim 10^{-5}$ and 10^{-8} , respectively, must be taken into account when accuracy requires it.
 - ix.* The three measured values for R_ℓ are consistent with lepton universality.
 - x.* Note the steep growth of the $e^+e^- \rightarrow W^+W^-$ cross-section in Fig. 16 when the gauge self-interactions are ignored.
 - xi.* Tevatron did not have enough statistical significance to claim ‘discovery’ of the Higgs boson.
 - xii.* The SM violates the conservation of baryon number non-perturbatively, thanks to a global U(1) anomaly, but in an amount that is not enough to explain the matter-antimatter asymmetry of the universe.
1. S. Weinberg, *The Quantum Theory of Fields. Vol. 1: Foundations*, Cambridge University Press, 2005.
 2. M. Schwartz, *Quantum Field Theory and the Standard Model*, Cambridge University Press, 2014.
 3. M. Maggiore, *A Modern Introduction to Quantum Field Theory*, Oxford University Press, 2005.
 4. A. Lahiri, P. B. Pal, *A first book of Quantum Field Theory*, Narosa Publishing House, 2nd edition, 2005.
 5. M. E. Peskin and D. V. Schroeder, *An Introduction to Quantum Field Theory*, Addison-Wesley, 1995.
 6. S. Pokorski, *Gauge Field Theories*, Cambridge University Press, 2nd edition, 2000.
 7. Y. Nambu, *Quasiparticles and Gauge Invariance in the Theory of Superconductivity*, *Phys. Rev.* **117** (1960) 648, <https://doi.org/10.1103/PhysRev.117.648>.
 8. J. Goldstone, *Field Theories with Superconductor Solutions*, *Nuovo Cim.* **19** (1961) 154, <https://doi.org/10.1007/BF02812722>.
 9. P. W. Anderson, *Plasmons, Gauge Invariance, and Mass*, *Phys. Rev.* **130** (1963) 439, <https://doi.org/10.1103/PhysRev.130.439>.
 10. F. Englert and R. Brout, *Broken Symmetry and the Mass of Gauge Vector Mesons*, *Phys. Rev. Lett.* **13** (1964) 321, <https://doi.org/10.1103/PhysRevLett.13.321>.
 11. P. W. Higgs, *Broken symmetries, massless particles and gauge fields*, *Phys. Lett.* **12** (1964) 132, [https://doi.org/10.1016/0031-9163\(64\)91136-9](https://doi.org/10.1016/0031-9163(64)91136-9).
 12. P. W. Higgs, *Broken Symmetries and the Masses of Gauge Bosons*, *Phys. Rev. Lett.* **13** (1964) 508, <https://doi.org/10.1103/PhysRevLett.13.508>.
 13. G. S. Guralnik, C. R. Hagen and T. W. B. Kibble, *Global Conservation Laws and Massless Particles*, *Phys. Rev. Lett.* **13** (1964) 585, <https://doi.org/10.1103/PhysRevLett.13.585>.
 14. P. W. Higgs, *Spontaneous Symmetry Breakdown without Massless Bosons*, *Phys. Rev.* **145** (1966) 1156, <https://doi.org/10.1103/PhysRev.145.1156>.
 15. T. W. B. Kibble, *Symmetry breaking in nonAbelian gauge theories*, *Phys. Rev.* **155** (1967) 1554, <https://doi.org/10.1103/PhysRev.155.1554>.
 16. G. 't Hooft and M. J. G. Veltman, *Regularization and Renormalization of Gauge Fields*, *Nucl. Phys. B* **44** (1972) 189, [https://doi.org/10.1016/0550-3213\(72\)90279-9](https://doi.org/10.1016/0550-3213(72)90279-9).
 17. S. L. Glashow, *Partial Symmetries of Weak Interactions*, *Nucl. Phys.* **22** (1961) 579, [https://doi.org/10.1016/0029-5582\(61\)90469-2](https://doi.org/10.1016/0029-5582(61)90469-2).
 18. S. Weinberg, *A Model of Leptons*, *Phys. Rev. Lett.* **19** (1967) 1264, <https://doi.org/10.1103/PhysRevLett.19.1264>.
 19. A. Salam, *Weak and Electromagnetic Interactions*, Proceedings of the 8th Nobel Symposium, 367-377 (1968). https://doi.org/10.1142/9789812795915_0034.
 20. M. Gell-Mann, *A Schematic Model of Baryons and Mesons*, *Phys. Lett.* **8** (1964) 214, [https://doi.org/10.1016/S0031-9163\(64\)92001-3](https://doi.org/10.1016/S0031-9163(64)92001-3).
 21. G. Zweig, *An SU(3) model for strong interaction symmetry and its breaking. Version 2*, Preprint CERN-TH-412 (1964).

22. H. Fritzsch, M. Gell-Mann and H. Leutwyler, *Advantages of the Color Octet Gluon Picture*, *Phys. Lett. B* **47** (1973) 365, [https://doi.org/10.1016/0370-2693\(73\)90625-4](https://doi.org/10.1016/0370-2693(73)90625-4).
23. N. Cabibbo, *Unitary Symmetry and Leptonic Decays*, *Phys. Rev. Lett.* **10** (1963) 531.
24. M. Kobayashi and T. Maskawa, *CP Violation in the Renormalizable Theory of Weak Interaction*, *Prog. Theor. Phys.* **49** (1973) 652, <https://doi.org/10.1143/PTP.49.652>
25. S. L. Glashow, J. Iliopoulos and L. Maiani, *Weak Interactions with Lepton-Hadron Symmetry*, *Phys. Rev. D* **2** (1970) 1285, <https://doi.org/10.1103/PhysRevD.2.1285>.
26. P. A. Zyla *et al.* [Particle Data Group], *Review of Particle Physics*, *PTEP* **2020** (2020) 083C01, <https://doi.org/10.1093/ptep/ptaa104>.
27. C. Jarlskog, *Commutator of the Quark Mass Matrices in the Standard Electroweak Model and a Measure of Maximal CP Violation*, *Phys. Rev. Lett.* **55** (1985) 1039. <https://doi.org/10.1103/PhysRevLett.55.1039>.
28. R. N. Mohapatra and P. B. Pal, *Massive neutrinos in physics and astrophysics. Second edition*, *World Sci. Lect. Notes Phys.* **60** (1998) 1; 72 1 (2004).
29. M. Gell-Mann, P. Ramond and R. Slansky, *Complex Spinors and Unified Theories*, *Conf. Proc. C* **790927** (1979) 315.
30. T. Yanagida, *Horizontal gauge symmetry and masses of neutrinos*, *Conf. Proc. C* **7902131** (1979) 95.
31. G. Hernández-Tomé, J. I. Illana and M. Masip, *The ρ parameter and $H^0 \rightarrow \ell_i \ell_j$ in models with TeV sterile neutrinos*, *Phys. Rev. D* **102** (2020) 113006 <https://doi.org/10.1103/PhysRevD.102.113006>.
32. B. Pontecorvo, *Mesonium and anti-mesonium*, *Sov. Phys. JETP* **6** (1957), 429.
33. Z. Maki, M. Nakagawa and S. Sakata, *Remarks on the unified model of elementary particles*, *Prog. Theor. Phys.* **28** (1962), 870-880. <https://doi.org/10.1143/PTP.28.870>.
34. B. Pontecorvo, *Neutrino Experiments and the Problem of Conservation of Leptonic Charge*, *Zh. Eksp. Teor. Fiz.* **53** (1967) 1717.
35. E. K. Akhmedov, *Do charged leptons oscillate?*, *JHEP* **09** (2007) 116 <https://doi.org/10.1088/1126-6708/2007/09/116>.
36. P. F. de Salas, D. V. Forero, S. Gariazzo, P. Martínez-Miravé, O. Mena, C. A. Ternes, M. Tórtola and J. W. F. Valle, *2020 global reassessment of the neutrino oscillation picture*, *JHEP* **02** (2021), 071 [https://doi.org/10.1007/JHEP02\(2021\)071](https://doi.org/10.1007/JHEP02(2021)071).
37. S. M. Bilenky and C. Giunti, *Neutrinoless Double-Beta Decay: a Probe of Physics Beyond the Standard Model*, *Int. J. Mod. Phys. A* **30** (2015) no.04n05, 1530001 <https://doi.org/10.1142/S0217751X1530001X>.
38. T. Hahn and M. Pérez-Victoria, *Automatized one loop calculations in four-dimensions and D-dimensions*, *Comput. Phys. Commun.* **118** (1999) 153 The *FeynArts* package can be downloaded from <http://www.feynarts.de>. [https://doi.org/10.1016/S0010-4655\(98\)00173-8](https://doi.org/10.1016/S0010-4655(98)00173-8).
39. T. Aoyama, T. Kinoshita and M. Nio, *Revised and Improved Value of the QED Tenth-Order Electron Anomalous Magnetic Moment*, *Phys. Rev. D* **97** (2018) 036001 <https://doi.org/10.1103/PhysRevD.97.036001>.
40. R. H. Parker, C. Yu, W. Zhong, B. Estey and H. Müller, *Measurement of the fine-structure constant as a test of the Standard Model*, *Science* **360** (2018) 191 <https://doi.org/10.1126/science.aap7706>.
41. L. Morel, Z. Yao, P. Cladé and S. Guellati-Khélifa, *Determination of the fine-structure constant with an accuracy of 81 parts per trillion*, *Nature* **588** (2020) 61-65. <https://doi.org/10.1038/s41586-020-2964-7>.
42. G. Arnison *et al.* [UA1], *Experimental Observation of Isolated Large Transverse Energy Electrons with Associated Missing Energy at $\sqrt{s} = 540$ GeV*, *Phys. Lett. B* **122** (1983), 103, [https://doi.org/10.1016/0370-2693\(83\)91177-2](https://doi.org/10.1016/0370-2693(83)91177-2).
43. M. Banner *et al.* [UA2], *Observation of Single Isolated Electrons of High Transverse Momentum in Events with Missing Transverse Energy at the CERN anti-p p Collider*, *Phys. Lett. B* **122** (1983) 476, [https://doi.org/10.1016/0370-2693\(83\)91605-2](https://doi.org/10.1016/0370-2693(83)91605-2).
44. G. Arnison *et al.* [UA1], *Experimental Observation of Lepton Pairs of Invariant Mass Around 95 GeV/c² at the CERN SPS Collider*, *Phys. Lett. B* **126** (1983) 398, [https://doi.org/10.1016/0370-2693\(83\)90188-0](https://doi.org/10.1016/0370-2693(83)90188-0).
45. P. Bagnaia *et al.* [UA2], *Evidence for $Z^0 \rightarrow e^+e^-$ at the CERN $\bar{p}p$ Collider*, *Phys. Lett. B* **129** (1983) 130, [https://doi.org/10.1016/0370-2693\(83\)90744-X](https://doi.org/10.1016/0370-2693(83)90744-X).
46. F. Abe *et al.* [CDF], *Observation of top quark production in $\bar{p}p$ collisions*, *Phys. Rev. Lett.* **74** (1995) 2626, <https://doi.org/10.1103/PhysRevLett.74.2626>.
47. S. Abachi *et al.* [D0], *Observation of the top quark*, *Phys. Rev. Lett.* **74** (1995) 2632, <https://doi.org/10.1103/PhysRevLett.74.2632>.
48. G. Aad *et al.* [ATLAS], *Observation of a new particle in the search for the Standard Model Higgs boson with the ATLAS detector at the LHC*, *Phys. Lett. B* **716** (2012) 1, <https://doi.org/10.1103/PhysRevLett.74.2632>.
49. S. Chatrchyan *et al.* [CMS], *Observation of a New Boson at a Mass of 125 GeV with the CMS Experiment at the LHC*, *Phys. Lett. B* **716** (2012) 30, <https://doi.org/10.1016/j.physletb.2012.08.021>.
50. F. J. Hasert *et al.* [Gargamelle Neutrino], *Observation of Neutrino Like Interactions Without Muon Or Electron in the Gargamelle Neutrino Experiment*, *Phys. Lett. B* **46** (1973), 138, [https://doi.org/10.1016/0370-2693\(73\)90499-1](https://doi.org/10.1016/0370-2693(73)90499-1).
51. R. L. Garwin, L. M. Lederman and M. Weinrich, *Observations of the Failure of Conservation of Parity and Charge Conjugation in Meson Decays: The Magnetic Moment of the Free Muon*, *Phys. Rev.* **105** (1957) 1415, <https://doi.org/10.1103/PhysRev.105.1415>.
52. C. S. Wu, E. Ambler, R. W. Hayward, D. D. Hoppes and R. P. Hudson, *Experimental Test of Parity Conservation in β Decay*, *Phys. Rev.* **105** (1957) 1413, <https://doi.org/10.1103/PhysRev.105.1413>.

53. T. D. Lee and C. N. Yang, *Question of Parity Conservation in Weak Interactions*, *Phys. Rev.* **104** (1956), 254, <https://doi.org/10.1103/PhysRev.104.254>.
54. E. Fermi, *An attempt of a theory of beta radiation. I.*, *Z. Phys.* **88** (1934) 161, <https://doi.org/10.1007/BF01351864>.
55. S. Schael *et al.* [ALEPH, DELPHI, L3, OPAL, SLD, LEP Electroweak Working Group, SLD Electroweak Group and SLD Heavy Flavour Group], *Precision electroweak measurements on the Z resonance*, *Phys. Rept.* **427** (2006) 257, <https://doi.org/10.1016/j.physrep.2005.12.006>.
56. P. Janot and S. Jadach, *Improved Bhabha cross section at LEP and the number of light neutrino species*, *Phys. Lett. B* **803** (2020) 135319, <https://doi.org/10.1016/j.physletb.2020.135319>.
57. S. Schael *et al.* [ALEPH, DELPHI, L3, OPAL and LEP Electroweak], *Electroweak Measurements in Electron-Positron Collisions at W-Boson-Pair Energies at LEP*, *Phys. Rept.* **532** (2013) 119, <https://doi.org/10.1016/j.physrep.2013.07.004>.
58. S. Weinberg, *On the Development of Effective Field Theory*, *Eur. Phys. J. H* **46** (2021) 6, <https://doi.org/10.1140/epjh/s13129-021-00004-x>.
59. C. H. Llewellyn Smith, *High-Energy Behavior and Gauge Symmetry*, *Phys. Lett. B* **46** (1973) 233, [https://doi.org/10.1016/0370-2693\(73\)90692-8](https://doi.org/10.1016/0370-2693(73)90692-8).
60. A. Djouadi, *The Anatomy of electro-weak symmetry breaking. I: The Higgs boson in the standard model*, *Phys. Rept.* **457** (2008) 1, <https://doi.org/10.1016/j.physrep.2007.10.004>.
61. D. de Florian *et al.* [LHC Higgs Cross Section Working Group], *Handbook of LHC Higgs Cross Sections: 4. Deciphering the Nature of the Higgs Sector*, <https://doi.org/10.23731/CYRM-2017-002>.
62. M. Aaboud *et al.* [ATLAS], *Observation of $H \rightarrow b\bar{b}$ decays and VH production with the ATLAS detector*, *Phys. Lett. B* **786** (2018) 59, <https://doi.org/10.1016/j.physletb.2018.09.013>.
63. A. M. Sirunyan *et al.* [CMS], *Evidence for Higgs boson decay to a pair of muons*, *JHEP* **01** (2021) 148, [https://doi.org/10.1007/JHEP01\(2021\)148](https://doi.org/10.1007/JHEP01(2021)148).
64. [ATLAS], *Measurements of Higgs boson properties in the diphoton decay channel with $36.1 \text{ fb}^{-1} \text{ pp}$ collision data at the center-of-mass energy of 13 TeV with the ATLAS detector*, ATLAS-CONF-2017-045 (2017).
65. [CMS], *Measurements of properties of the Higgs boson in the four-lepton final state in proton-proton collisions at $\sqrt{s} = 13 \text{ TeV}$* , CMS-PAS-HIG-19-001 (2019).
66. M. Awramik, M. Czakon and A. Freitas, *Electroweak two-loop corrections to the effective weak mixing angle*, *JHEP* **11** (2006) 048, <https://doi.org/10.1088/1126-6708/2006/11/048>.
67. G. W. Bennett *et al.* [Muon g-2], *Final Report of the Muon E821 Anomalous Magnetic Moment Measurement at BNL*, *Phys. Rev. D* **73** (2006) 072003, <https://doi.org/10.1103/PhysRevD.73.072003>.
68. T. Aoyama, N. Asmussen, M. Benayoun, J. Bijnens, T. Blum, M. Bruno, I. Caprini, C. M. Carloni Calame, M. Cè and G. Colangelo, *et al.* *The anomalous magnetic moment of the muon in the Standard Model*, *Phys. Rept.* **887** (2020) 1, <https://doi.org/10.1016/j.physrep.2020.07.006>.
69. B. Abi *et al.* [Muon g-2], *Measurement of the Positive Muon Anomalous Magnetic Moment to 0.46 ppm*, *Phys. Rev. Lett.* **126** (2021) 141801, <https://doi.org/10.1103/PhysRevLett.126.141801>.
70. R. Aaij *et al.* [LHCb], *Test of lepton universality in beauty-quark decays*,
71. J. Albrecht, D. van Dyk and C. Langenbruch, *Flavour anomalies in heavy quark decays*, *Prog. Part. Nucl. Phys.* **120** (2021) 103885, <https://doi.org/10.1016/j.pnpnp.2021.103885>.
72. E. Kou *et al.* [Belle-II], *The Belle II Physics Book*, *PTEP* **2019** (2019) 123C01, [erratum: *PTEP* **2020** (2020) 029201], <https://doi.org/10.1093/ptep/ptz106>.
73. J. Haller, A. Hoecker, R. Kogler, K. Mönig, T. Peiffer and J. Stelzer, *Update of the global electroweak fit and constraints on two-Higgs-doublet models*, *Eur. Phys. J. C* **78** (2018) 675, <https://doi.org/10.1140/epjc/s10052-018-6131-3>.
74. V. A. Kuzmin, V. A. Rubakov and M. E. Shaposhnikov, *On the Anomalous Electroweak Baryon Number Nonconservation in the Early Universe*, *Phys. Lett. B* **155** (1985) 36, [https://doi.org/10.1016/0370-2693\(85\)91028-7](https://doi.org/10.1016/0370-2693(85)91028-7).
75. S. Davidson, E. Nardi and Y. Nir, *Leptogenesis*, *Phys. Rept.* **466** (2008) 105, <https://doi.org/10.1016/j.physrep.2008.06.002>.
76. G. Bertone, D. Hooper and J. Silk, *Particle dark matter: Evidence, candidates and constraints*, *Phys. Rept.* **405** (2005) 279, <https://doi.org/10.1016/j.physrep.2004.08.031>.
77. S. Clesse and J. García-Bellido, *Seven Hints for Primordial Black Hole Dark Matter*, *Phys. Dark Univ.* **22** (2018), 137, <https://doi.org/10.1016/j.dark.2018.08.004>.
78. R. D. Peccei, *The Strong CP problem and axions*, *Lect. Notes Phys.* **741** (2008) 3, https://doi.org/10.1007/978-3-540-73518-2_1.
79. P. J. E. Peebles and B. Ratra, *The Cosmological Constant and Dark Energy*, *Rev. Mod. Phys.* **75** (2003) 559, <https://doi.org/10.1103/RevModPhys.75.559>.
80. N. Aghanim *et al.* [Planck], *Planck 2018 results. VI. Cosmological parameters*, *Astron. Astrophys.* **641** (2020) A6; [erratum: *Astron. Astrophys.* **652** (2021) C4] <https://doi.org/10.1051/0004-6361/201833910>.
81. S. P. Martin, *A Supersymmetry primer*, *Adv. Ser. Direct. High Energy Phys.* **18** (1998) 1, <https://doi.org/10.1142/9789812839657-0001>.
82. N. Arkani-Hamed, S. Dimopoulos and G. R. Dvali, *The Hierarchy problem and new dimensions at a millimeter*, *Phys. Lett. B* **429** (1998) 263, [https://doi.org/10.1016/S0370-2693\(98\)00466-3](https://doi.org/10.1016/S0370-2693(98)00466-3).

83. L. Randall and R. Sundrum, *A Large mass hierarchy from a small extra dimension*, *Phys. Rev. Lett.* **83** (1999) 3370, <https://doi.org/10.1103/PhysRevLett.83.3370>.
84. W. Buchmuller and D. Wyler, *Effective Lagrangian Analysis of New Interactions and Flavor Conservation*, *Nucl. Phys. B* **268** (1986) 621, [https://doi.org/10.1016/0550-3213\(86\)90262-2](https://doi.org/10.1016/0550-3213(86)90262-2).
85. B. Grzadkowski, M. Iskrzynski, M. Misiak and J. Rosiek, *Dimension-Six Terms in the Standard Model Lagrangian*, *JHEP* **10** (2010) 085, [https://doi.org/10.1007/JHEP10\(2010\)085](https://doi.org/10.1007/JHEP10(2010)085).
86. J. Ellis, M. Madigan, K. Mimasu, V. Sanz and T. You, *Top, Higgs, Diboson and Electroweak Fit to the Standard Model Effective Field Theory*, *JHEP* **04** (2021) 279, [https://doi.org/10.1007/JHEP04\(2021\)279](https://doi.org/10.1007/JHEP04(2021)279).